

Appendix 12

Description and validation of hydrodynamic and wave models for dredging and spoil disposal



HR Wallingford
Working with water

EX 6218

Ichthys Gas Field Development Project Description and validation of hydrodynamic and wave models for dredging and spoil disposal



Report EX 6218

INPEX Document number: C036-AH-REP-0071

Release 3.0

February 2010



Document Information

Project	Ichthys Gas Field Development Project
Report title	Description and validation of hydrodynamic and wave models for dredging and spoil disposal
Client	INPEX
Client Representative	Harotushi Usui
Project No.	EBR4470
Report No.	EX 6218
INPEX Document No.	C036-AH-REP-0071
Project Manager	S R Richardson
Project Director	C W Skipper

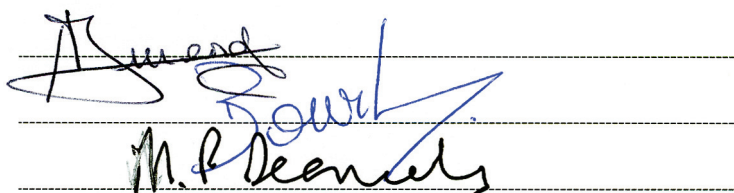
Document History

Date	Release	Prepared	Approved	Authorised	Notes
14/01/10	1.0	NDU	SBO	MPD	Preliminary draft report
10/02/10	2.0	NDU	SBO	MPD	Final draft report
26/02/10	3.0	NDU	SBO	MPD	Final report

Prepared

Approved

Authorised



Handwritten signatures for Prepared, Approved, and Authorised, each on a dashed line.

© HR Wallingford Limited

HR Wallingford accepts no liability for the use by third parties of results or methods presented in this report. The Company also stresses that various sections of this report rely on data supplied by or drawn from third party sources. HR Wallingford accepts no liability for loss or damage suffered by the client or third parties as a result of errors or inaccuracies in such third party data.

This report may be cited as:

HR Wallingford. 2010. *Ichthys Gas Field Development Project: description and validation of hydrodynamic and wave models for dredging and spoil disposal*. Report prepared for INPEX Browse, Ltd., Perth, Western Australia.

Summary

Ichthys Gas Field Development Project

Description and validation of hydrodynamic and wave models for dredging and spoil disposal

Report EX6218

February 2010

INPEX Browse, Ltd. (INPEX) proposes to develop the natural gas and associated condensate contained in the Ichthys Field situated about 220 km off Western Australia's Kimberley coast and about 820 km west south west of Darwin. HR Wallingford is providing support to INPEX with this regard and was commissioned to carry out numerical modelling work associated with INPEX's preparation of the EIS. This technical report, *Description and validation of hydrodynamic and wave models for dredging and spoil disposal*, was prepared in part fulfilment of that commission. The sediment plume dispersion modelling and development of the dredging plan is the subject of a separate document (INPEX Report No C036-AH-REP-0067).

The dispersion of material released either during the extraction or placement phases of the dredge cycle is primarily governed by the prevailing hydrodynamics. An effective hydrodynamic model is paramount to the accurate representation of the advection and diffusion of material released into the water column. The starting point for the sediment plume dispersion modelling was therefore to develop regional numerical models of currents and waves. The establishment of these models is described in this report.

The comparisons of the flow model results against both time histories of water surface elevations and observed current data give confidence in the flow model predictions and their use to investigate the potential dispersion of sediment from the main subtidal areas of the East Arm where the dredging activities will take place. The comparisons of the wave model results against observed wave data indicate that the model tends to under-predict the wave heights in the approaches to Darwin Harbour, but it generally reproduces them well at the dredging site. It may be important to remember that wave activity is naturally limited in the East Arm.

Additional analyses were performed to determine the sensitivity of the flow model results to the mangrove friction coefficients and to the meteorological conditions. These analyses indicated that the hydrodynamics in Darwin Harbour are relatively insensitive to the physical representation of the vegetation in the model, although the tidal volume it covers is critical. They also showed that typical wind conditions have a very limited impact on both water levels and velocities. Their impact is more pronounced for more extreme conditions. The assumptions made in this study are therefore deemed appropriate.

Contents

<i>Title page</i>	<i>i</i>
<i>Document Information</i>	<i>ii</i>
<i>Summary</i>	<i>iii</i>
<i>Contents</i>	<i>v</i>

1.	Introduction.....	1
1.1	Background.....	1
1.2	Objectives of study.....	1
1.3	Key assumptions.....	2
1.4	approach to study.....	2
1.5	Report structure.....	3
2.	Numerical model set up.....	4
2.1	Numerical model extent.....	4
2.2	Numerical model discretisation.....	4
2.3	Numerical model bathymetry.....	5
2.4	Numerical solvers.....	5
2.5	Boundary conditions for the flow model.....	5
2.6	Boundary conditions for the wave model.....	6
2.7	Meteorological conditions.....	7
3.	Calibration-validation of the flow model.....	8
3.1	Flow calibration parameter.....	8
3.2	Selected events.....	8
3.3	Flow model result comparison.....	10
4.	Calibration-validation of the wave model.....	13
4.1	Wave calibration parameter.....	13
4.2	Selected events.....	13
4.3	Wave model result comparison.....	14
5.	Application of the flow model.....	15
5.1	Boundary conditions for the flow model.....	15
5.2	Meteorological conditions.....	16
5.3	Sensitivity analysis: mangrove friction coefficients.....	16
5.4	Sensitivity analysis: meteorological conditions.....	17
6.	Conclusions.....	19
7.	References.....	20

Tables

Table 1	Spring and neap tidal ranges published for Darwin.....	8
Table 2	Locations where velocity observations are available (see Figure 4).....	9
Table 3	Locations where water depth observations are available (see Figure 6).....	10
Table 4	Locations where published levels are available (see Figure 2).....	10
Table 5	Level differences between model predictions and measured values.....	11
Table 6	Speed differences between model predictions and measured values.....	12
Table 7	Locations where wave observations are available (see Figure 2).....	13

Contents continued

Table 8	Spring and neap tidal ranges, HAT and LAT at Darwin.....	16
Table 9	Wind conditions applied in the model	16
Table 10	Effect of the friction coefficient in the mangroves on levels and speeds.....	17
Table 11	Effect of meteorological conditions on levels and speeds	18
Table 12	Surge as a result of meteorological conditions	18

Figures

Figure 1	Geographic location of Darwin Harbour
Figure 2	Model extent, mesh resolution and available datasets, View of Beagle Gulf
Figure 3	Bathymetry of the flow and wave models, View of Beagle Gulf
Figure 4	Numerical model mesh resolution and available datasets, Close-up view of Darwin Harbour
Figure 5	Bathymetry of the flow and wave models, Close-up view of Darwin Harbour
Figure 6	Model mesh resolution and available datasets, Close-up view of Blaydin Point
Figure 7	Annual offshore wave climate and wave rose, NOAA Data Point
Figure 8	Wet season offshore wave climate and wave rose, NOAA Data Point
Figure 9	Dry season offshore wave climate and wave rose, NOAA Data Point
Figure 10	Annual offshore wind climate and wind rose, NOAA Data Point
Figure 11	Wet season offshore wind climate and wind rose, NOAA Data Point
Figure 12	Dry season offshore wind climate and wind rose, NOAA Data Point
Figure 13	Water level at Cape Hotham, Differences in published data (Mike-21 / C-Map)
Figure 14	Water level at Tapa Bay, Model comparison against C-Map data
Figure 15	Water level at Darwin, Model comparison against C-Map data
Figure 16	Water level at Night Cliff, Model comparison against C-Map data
Figure 17	Water level at Gauge 1, Model comparison against observed data
Figure 18	Water level at Gauge 2, Model comparison against observed data
Figure 19	Water level at Gauge 3, Model comparison against observed data
Figure 20	Water level at Gauge 4, Model comparison against observed data
Figure 21	Current speed at Monitor 1, Model comparison against observed data
Figure 22	Current direction at Monitor 1, Model comparison against observed data
Figure 23	Current speed at Sentinel 1, Model comparison against observed data
Figure 24	Current direction at Sentinel 1, Model comparison against observed data
Figure 25	Current speed at Monitor 2, Model comparison against observed data
Figure 26	Current direction at Monitor 2, Model comparison against observed data
Figure 27	Current speed at Sentinel 2, Model comparison against observed data
Figure 28	Current direction at Sentinel 2, Model comparison against observed data
Figure 29	Current speed at Sentinel 3, Model comparison against observed data
Figure 30	Current direction at Sentinel 3, Model comparison against observed data
Figure 31	Current speed distribution and tidal ellipse at Monitor 1, Model comparison against observed data
Figure 32	Current speed distribution and tidal ellipse at Sentinel 1, Model comparison against observed data
Figure 33	Current speed distribution and tidal ellipse at Monitor 2, Model comparison against observed data
Figure 34	Current speed distribution and tidal ellipse at Sentinel 2, Model comparison against observed data
Figure 35	Current speed distribution and tidal ellipse at Sentinel 3, Model comparison against observed data
Figure 36	Significant wave height, Model comparison against observed data
Figure 37	Absolute peak period, Model comparison against observed data

Contents continued

Appendices

- Appendix 1 Numerical wave and flow solvers
- Appendix 2 Characterisation of the Darwin Harbour mangrove

1. Introduction

1.1 BACKGROUND

INPEX Browse, Ltd. (INPEX) proposes to develop the natural gas and associated condensate contained in the Ichthys Field situated about 220 km off Western Australia's Kimberley coast and about 820 km west south west of Darwin. The field encompasses an area of 800 km² in water depths ranging from 235 to 275 m.

The two reservoirs which make up the field are estimated to contain 12.8 tcf (trillion cubic feet) of sales gas and 527 MMbbl (million barrels) of condensate. INPEX proposes to process the reservoir fluids to produce liquefied natural gas (LNG), liquefied petroleum gases (LPGs) and condensate for export to overseas markets.

For the Ichthys Project, the company plans to install offshore extraction facilities at the field and a subsea gas pipeline from the field to onshore facilities at Blaydin Point in Darwin Harbour. A two train LNG plant, an LPG fractionation plant, a condensate stabilisation plant and a product loading jetty will be constructed at a site on Blaydin Point. Around 85% of the condensate will be extracted and exported directly from the offshore facilities while the remaining 15% will be processed at and exported from Blaydin Point.

In May 2008 INPEX referred its proposal to develop the Ichthys Field to the Commonwealth's Department of the Environment, Water, Heritage and the Arts and the Northern Territory's Department of Natural Resources, Environment and the Arts. The Commonwealth and Northern Territory ministers responsible for environmental matters both determined that the Project should be formally assessed at the environmental impact statement (EIS) level to ensure that potential impacts associated with the Project are identified and appropriately addressed.

Assessment will be undertaken in accordance with the *Environment Protection and Biodiversity Conservation Act 1999* (Cwlth) and the *Environmental Assessment Act* (NT). It was agreed that INPEX should submit a single EIS document to the two responsible government departments in the Northern Territory and the Commonwealth for assessment.

HR Wallingford Limited was commissioned to carry out modelling work associated with INPEX's preparation of the EIS and this technical report, *Description and validation of hydrodynamic and wave models for dredging and spoil disposal*, was prepared in part fulfilment of that commission.

1.2 OBJECTIVES OF STUDY

HR Wallingford was commissioned to conduct numerical modelling of the dredging and disposal associated with the proposed dredging activities within Darwin Harbour. This also required the development of the Dredging Case Study. The development of the Dredging Case Study is subject of a separate report and is covered in INPEX Document No. C036-AH-REP-0067.

The starting point for the sediment transport dispersion modelling is to develop regional numerical models of currents and waves, whose results are used to drive both the fine

and coarse grained sediment transport models. The establishment of these models is described in this report.

The sediment plume dispersion modelling and development of the dredging plan is the subject of a separate report (EX6219).

1.3 KEY ASSUMPTIONS

The water level in Darwin Harbour is driven by the tidal variations of the Beagle Gulf. The amplitude of the oscillations varies between about 2 m (neap tides) and over 7 m (spring tides). It is anticipated that the tidal oscillations would drive salt waters into all the arms and creeks of Darwin Harbour. The volume of water entering the harbour is such that it is appropriate to assume that the water column is well mixed at the proposed dredging site. This may not be true further upstream in East Arm, particularly following a heavy rainfall event. The numerical modelling study was therefore carried out with a 2D hydrodynamic model.

Wave data were collected on behalf of INPEX within Darwin Harbour. They indicate that there is only a limited amount of wave energy entering the harbour from the Beagle Gulf. Most of the wave activity at Blaydin Point is generated locally within the East Arm, yielding short period waves of limited height. This was corroborated by the wave transformation model (Section 4).

In this study the sediment transport modelling for fines and sands released in the Darwin Harbour by dredging was therefore driven by tidal currents and wind-generated waves only. For fines and sands released at the offshore disposal ground, sensitivity tests were undertaken to demonstrate the significance of wave effects on the expected transport patterns.

The analysis of the data provided by INPEX within Darwin Harbour yielded a map of spatially-varying friction coefficients in the mangroves, according to the types of vegetation, their assumed density and strength. This analysis is presented in Appendix 2. Best judgment was used to derive sensible coefficients based on the existing literature and a sensitivity analysis to the value of the friction coefficient in the mangroves was conducted (Section 5.3).

1.4 APPROACH TO STUDY

Upon gathering and review of existing sources of data, a suite of regional numerical models was developed (including a 2D hydrodynamic model and a 3rd generation wave transformation model) to cover the Beagle Gulf and the Darwin Harbour, with particular emphasis in Darwin Harbour East Arm. The models deemed the most suitable were selected from HR Wallingford's suite of models. Their calibration and validation were achieved through the experience and expertise of the project team.

The approach to the sediment plume dispersion modelling has been to simulate the entire dredging operation via a number of representative phases. A typical dredge phase covers a time period of 1 to 11 months; the whole operation is made up of 10 phases. The hydrodynamics for a particular phase are represented by a repeating spring-neap cycle of tides representative of the wet or dry season and a time-series of wind data from which to generate local wind waves. The influence of wind waves are particularly important over the intertidal areas, where they contribute to the redistribution of fines from the lower intertidal mudflats into the mangrove areas. The model bathymetry is

selected to be representative of conditions during the phase and thus over time the evolution of the dredged footprint is gradually included. The sediment plume dispersion modelling runs one phase then the next until the whole of the dredging operation is simulated. This approach has the merits of being computationally efficient to set up and to run thus enabling several different alternative dredging strategies to be simulated and sensitivity tests to key assumptions to be carried out.

1.5 REPORT STRUCTURE

This report describes the calibration and validation of the hydrodynamic and wave models of Darwin Harbour. It also presents the application of the hydrodynamic model to provide input to the sediment transport model.

This report is structured as follows:

Section 1 – Introduction

Section 2 – Numerical model set up

Section 3 – Calibration-validation of the flow model

Section 4 – Calibration-validation of the wave model

Section 5 – Application of the flow model to provide input to the sediment transport model

Section 6 – Conclusions

Section 7 – References

Appendices to this report include descriptions of the software used and the approach to representation of the mangrove areas in the numerical model.

2. Numerical model set up

A numerical model of the Beagle Gulf and Darwin Harbour was set up in this study to determine both the hydrodynamic and wave conditions at the entrance of the harbour and in the East Arm.

In the remainder of this document the terms *flow model* and *wave model* will be used to refer to the hydrodynamic and wave transformation models based on the numerical representation detailed hereafter.

The coordinate system used in this study was the Map Grid of Australia (MGA), zone 52, based on the Geocentric Datum of Australia 1994 (GDA94). The vertical datum was Mean Sea Level (MSL).

2.1 NUMERICAL MODEL EXTENT

The model extends for over 200 km along the coast from Point Jenny to Cape Hotham. West of the study area, it extends offshore to approximately the 50 m contour, near the closest NOAA WAVEWATCH III™ global wave model at 12°S 130°E (Ref. 1) (hereinafter referred to as NOAA Data Point) and therefore covers Beagle Gulf. North of the study area, it extends to the southern coastline of Melville and Bathurst Islands. East of the study area, it extends to Cape Hotham and therefore includes Clarence Straits.

The model coverage is such that it enables representation of the offshore spoil disposal ground and the overall transport of the sediment plumes.

In addition, a particular focus of the sediment plume dispersion modelling is to consider the potential for sediment accretion over the mangrove areas of Darwin Harbour. The numerical model area therefore includes the mangroves, as identified from georeferenced contour data supplied by INPEX (Ref. 2). Additional information with respect to how the mangroves were accounted for in the model is presented in Appendix 2 of this report.

The model area and mesh resolution are shown in Figure 2.

2.2 NUMERICAL MODEL DISCRETISATION

A triangular finite element mesh with spatially varying resolution was used to represent the model area. The edge length of the triangles varied from 1500 m away from the harbour, to 350 m across Darwin Harbour approaches and about 50 m at the proposed dredging site and at the shoreline between Channel Island and the mouth of the Elizabeth River. For the pipeline approach a resolution of 30 m was specified across, with 100 m used at the offshore disposal site. Overall, the model area was represented using approximately 48,000 nodes and 92,000 triangles. The model area and mesh resolution are shown in Figure 2 superimposed on a satellite image obtained from Google Earth. Close-up views of the mesh are shown in Figure 4 for the Darwin Harbour and in Figure 6 in the vicinity of INPEX facilities.

The locations where the flow and wave models have been calibrated and verified (Sections 3 and 4) are identified in these three figures.

2.3 NUMERICAL MODEL BATHYMETRY

The bathymetric data used to set up the numerical model comprised the most recent available information:

- Bathymetric contours and spot heights from the C-Map electronic chart database covering the Beagle Gulf and Clarence Straits,
- Bathymetric data collected in May and June 2008 on behalf of *Asia-Pacific ASA Pty Ltd.* (APASA), in Port Darwin with particular emphasis in the intertidal areas and approach channel. It is important to note that these data were supplied as water depths. They were subsequently corrected by HR Wallingford based on water surface elevations observed at Darwin Harbour for the same period (source: Australian Government, Bureau of Meteorology, Ref. 3) to yield sea bed elevations. After correction it was verified that the data generally tied in with the C-Map data as well as the topographic data.
- Topographic data obtained from the U.S. Geological Survey at 90 m spatial resolution covering Melville and Bathurst Islands as well as all the smaller islands in the Beagle Gulf and Van Diemen Gulf, and covering the mainland between Point Jenny and Finke Bay approximately. The reference elevation datum for these data was ascertained by relating matching the MSL and MHWS water lines. These data were particularly relevant to improve the representation of the intertidal areas in the model.

A digital elevation model of the sea bed throughout the model area, including intertidal and mangrove areas, was constructed by combining data from the sources described above. Best judgement was used to extrapolate in areas where sparse or no data were available. The resulting seabed map is presented in Figure 3 for the whole model. A close-up view of Darwin Harbour is shown in Figure 5.

Close analysis of detailed Fugro bathymetry survey data in the Darwin Harbour (Ref. 4) concluded that these data were in good agreement with the developed model bathymetry.

2.4 NUMERICAL SOLVERS

Flow conditions in the area of interest were predicted using the TELEMAC-2D hydrodynamic solver. The flow model was set up and validated against a selection of available in-situ measurements. This is the subject of Section 3.

Wave conditions in the area of interest were predicted using the TOMAWAC third generation wave transformation solver based on the same mesh used for the flow model. The wave model was set up and validated against a selection of available in-situ measurements. This is the subject of Section 4.

Both TELEMAC-2D and TOMAWAC are part of the same modelling system, a description of which can be found in Appendix 1.

2.5 BOUNDARY CONDITIONS FOR THE FLOW MODEL

TELEMAC-2D is driven by currents and/or water levels. In this study, time-varying water levels were applied along the offshore boundaries of the flow model. The water

levels were derived from data obtained from the C-Map database at a half hour resolution at a tidal station (secondary port) along the eastern model boundary and from the Mike-21 global model data also at a half hour resolution at discrete locations along the western model boundary (Ref. 5).

Along the eastern boundary a sensitivity analysis was performed to the source of tidal level data to determine the most appropriate data set for the project site. The tidal range obtained from the Mike-21 global model at Cape Hotham was significantly different from that obtained from the C-Map database (Figure 13), which highlighted the difficulty of obtaining accurate level data in the Clarence Straits. The results of the sensitivity analysis indicated that the Mike-21 global model data were not appropriate for the eastern model boundary; through comparison with observed data, water levels within Darwin Harbour were more accurately predicted under C-Map conditions than under Mike-21 global model conditions.

Along the western model boundary, however, it was necessary to use the data from the Mike-21 global model because of the limited number of tidal stations (secondary ports) available through the C-Map database for the northern coast of Australia. Although it was envisaged that to move the location of the western boundary would be defined to match these few ports, the resulting boundary alignment and proximity to the site of interest were not satisfactory.

Best judgement was used to derive appropriate interpolation of water levels across the model boundaries from the data obtained at discrete locations. It should, however, be noted that the data obtained from either the Mike-21 global model or the C-Map database are based on a limited number of harmonic (tidal) constituents, which may restrict the accuracy of the flow model results. It is therefore anticipated that flow patterns within Beagle Gulf, away from the locations where measurement points were provided to HR Wallingford in Darwin Harbour, might not be as well calibrated as within Darwin Harbour.

2.6 BOUNDARY CONDITIONS FOR THE WAVE MODEL

Offshore wave conditions obtained from the NOAA Data Point were used as boundary conditions to the wave model. The dataset consists of a three-hourly time-series of wave and wind conditions covering a period from January 1997 to July 2009 inclusive. The annual and seasonal offshore wave climates and wave roses derived from these data are presented in Figures 7, 8 and 9 respectively. A rose is a visual representation of the frequency of occurrence of certain conditions, discretised into directional sectors and wave height bins. In this case each ring on the rose represents a frequency of occurrence of 10%. The width of the colour bars represents the frequency of occurrence of a wave height from a given direction and within a certain range.

Two-dimensional wave spectra were applied along the wave model western boundary. These spectra were computed by approximating the total wave conditions predicted at the NOAA Data Point by a JONSWAP spectrum. No wave conditions were applied along the wave model eastern boundary. This was considered to be an appropriate approximation since waves generated/propagated in the Van Diemen Gulf would be blocked off to some extent by the islands across the Clarence Straits.

2.7 METEOROLOGICAL CONDITIONS

In the absence of long-term site-specific wind data, the offshore wind time record obtained from the NOAA Data Point was used. Figure 10 presents the annual offshore wind climate derived from these data using 1 m/s wind speed bins and 30° direction sectors. The data are expressed in parts per hundred thousand, based on the entire wind record. Figure 11 and Figure 12 present seasonal wind climates (wind speed against wind direction) for the wet and dry seasons respectively. These figures also present the offshore wind climates in the form of annual and seasonal wind roses.

When meteorological conditions were considered in the flow and/or wave models, the winds were blown over the entire model area (spatially and temporally constant wind field).

It should be noted that the sediment plume dispersion modelling wind data was extracted from the NOAA Data Point. This provided a complete representative wet and dry season time-series (12 month at 3-hourly resolution) wind data set that was applied to generate local waves within Darwin Harbour.

3. Calibration-validation of the flow model

3.1 FLOW CALIBRATION PARAMETER

In TELEMAC-2D the bottom roughness can be represented with a linear coefficient, a Chézy, Strickler / Manning coefficient, or using a Nikuradse roughness length. A Chézy formulation was used for this study. The use of different coefficients was investigated as part of the flow model sensitivity testing and calibration. A spatially-varying coefficient was eventually used, dependent on the local water depth. Values between 120 and 70 were used throughout the model, in the main body of water, below MSL. These values are within the range of expected bottom roughness coefficients.

Best judgment was used to derive sensible coefficients in the mangroves, based on the existing literature and the types of vegetation (Appendix 2). A sensitivity analysis was also conducted in this study to investigate the impact of the mangrove friction coefficient on levels and velocities in the main channels. The results of this analysis are presented in Section 5.3.

3.2 SELECTED EVENTS

The flow model of Darwin Harbour was calibrated before being applied to provide the flow fields required as input to the wave model and for the sediment transport modelling to define the flows at the dredging site. Calibration-validation was carried out using observed current and water level data over complete 15-day tidal cycles:

- April 25th to May 10th, 2008 inclusive,
- May 20th to June 4th, 2008 inclusive,
- June 23rd to July 8th, 2008 inclusive, and
- July 22nd to August 6th, 2008 inclusive.

Calibration-validation against a complete 15-day cycle, as opposed to calibration against one tide event alone, enhances the accuracy of the exercise. It was further improved by considering four 15-day periods. The flow data had not been surveyed concurrently at all observation sites but in sequence.

Table 1 puts the four calibration-validation periods in context with respect to 20-year average / low / high tidal ranges derived from water level data published for Darwin (Ref. 3).

Table 1 Spring and neap tidal ranges published for Darwin

	Spring tidal range (m)	Neap tidal range (m)
20-year average	5.74	1.95
20-year low	4.08	0.67
20-year high	7.09	3.78
Calibration period 1	6.09	1.48
Calibration period 2	5.30	2.36
Calibration period 3	5.58	2.95
Calibration period 4	5.93	2.64

It is important for any tidal model to be able to predict accurately the attenuation or amplification of water level fluctuations throughout the model domain, and also to predict the arrival time of the tidal wave. Good agreement between the observed tidal level and the simulated water levels shows that the dynamics of the tide are well represented in the flow model.

For calibration-validation purposes, depth-averaged current speeds and directions predicted by the flow model were compared against *Acoustic Doppler Current Profiler* (ADCP) mooring data collected by INPEX at five sites in the area of interest. The locations of these points (Monitor 1 and 2 and Sentinel 1 to 3) are marked by half-filled triangles in Figure 4; their coordinates are given in Table 2. All instruments were deployed in approximately 12.5 m water depth.

Table 2 Locations where velocity observations are available (see Figure 4)

MGA Zone 52		
Coordinates		
	(E)	(N)
Monitor 1	699681.8	8618941.4
Sentinel 1	705239.3	8616517.4
Monitor 2	696284.7	8625206.5
Sentinel 2	696357.1	8619852.5
Sentinel 3	692723.6	8624754.1

The first ADCP moorings were deployed on April 15th, 2008 at Sentinel 1 and Monitor 1 locations and recovered on May 12th, 2008. Monitor 2 ADCP mooring was installed between May 16th and June 5th, 2008; Sentinel 2 mooring between June 11th and July 15th, 2008; and Sentinel 3 mooring between July 15th and August 13th, 2008.

The ADCP current data were collected every 10 or 20 minutes depending on location. The instruments were set to measure the current characteristics every 50 cm or less (35 cm at Sentinel 3) throughout the water column. Typically, surface flows are not measured by ADCP devices. The measured current speeds and directions were subsequently analysed by HR Wallingford to yield depth-averaged values at all observation locations.

The observed tidal currents generally respond to the local bathymetry:

- At Sentinel 3, near the entrance to the harbour, the flood current sets in a south-easterly direction and attains a maximum speed of about 1.0 m/s for a spring tide, and 0.3 m/s for a neap tide. The ebb sets in a northerly direction with a maximum speed of about 1.6 m/s for a spring tide and 0.5 m/s for a neap tide.
- On the other side of the channel, at Monitor 2, the current speeds do not exhibit such noticeable variations between the ebb and flood cycles as was the case at Sentinel 3. The flood current sets in a general south-south-easterly direction while the ebb sets in a northerly direction. The current speed reaches 0.9-1.0 m/s for a spring tide; and 0.3 m/s for a neap tide.
- At Sentinel 2, the flood current sets in a south-easterly direction and the ebb current sets in a north-westerly direction. The current speed reaches 1.2-1.3 m/s for a spring tide and 0.4 m/s for a neap tide.

- At the split between the East and Middle Arms, at Monitor 1, the flood current generally sets in an east-south-easterly direction, the ebb in a north-westerly direction. There is, however, a significant amount of spreading about the main tidal axis. For a spring tide, the flood current speed reaches 0.9 m/s; the ebb current speed reaches 0.7 m/s. For a neap tide the currents are very weak, around 0.1 m/s.
- The current speeds at Sentinel 1 are of the same order as those at Monitor 1; but contrarily to Monitor 1, the directions are here tightly distributed along the main axis. The flood current sets in an east-south-easterly direction and the ebb in a west-north-westerly direction.

Pressure (water depth) data were collected in the intertidal areas within Port Darwin East Arm concurrently with the current data (May 15th to June 10th, 2008). This gives tidal height information at the site, which was used to validate the flow model. The locations of these points (Tidal gauges 1 to 4) are marked by stars in Figure 6; their coordinates are given in Table 3. Wave data were also collected as part of this field measurement campaign and are discussed in Section 4.1.

Table 3 Locations where water depth observations are available (see Figure 6)

MGA Zone 52 Coordinates		
	(E)	(N)
Gauge 1	708228.2	8616843.2
Gauge 2	705147.4	8616336.7
Gauge 3	705128.4	8616220.0
Gauge 4	708204.2	8616446.9

3.3 FLOW MODEL RESULT COMPARISON

Calibration-validation of the flow model was achieved through a comparison of predicted water levels against water levels observed near the dredging site, and against published levels at locations Darwin, Night Cliff and Tapa Bay (Ref. 3).

Additional comparison of predicted current velocities (amplitude and direction) against current velocities observed in April-August 2008 was also performed.

The locations of the calibration sites are marked by stars in Figure 2 (published level data) and in Figure 6 (observed level data) and by half-filled triangles in Figure 4 (observed velocity data); the coordinates of the points where measurements were made have been reported in Section 3.2; the coordinates of the points where only published levels were available are given below in Table 4.

Table 4 Locations where published levels are available (see Figure 2)

MGA Zone 52 Coordinates		
	(E)	(N)
Darwin	701359.8	8620761.5
Night Cliff	699269.2	8630448.9
Tapa Bay	673070.3	8624144.1

Figure 14 to Figure 20 present time histories of water surface elevations predicted by the flow model for each 15-day calibration-validation period (thick orange line), compared to the observed levels (blue crosses) for the same period.

Similarly Figure 21, Figure 23, Figure 25, Figure 27 and Figure 29 present time histories of predicted (thick orange line) and observed (blue crosses) current speeds at all the calibration sites and for the various calibration-validation periods. Figure 22, Figure 24, Figure 26, Figure 28 and Figure 30 present time histories of current directions. The comparison of current velocities is also presented in Figure 31 to Figure 35 in the form of tidal ellipses. A tidal ellipse is a visual representation of the direction and strength of the flow throughout one or more tidal cycles and gives a good indication of the major current axis. The rings on the ellipse represent the current speed (0.5 m/s interval in Figure 31 to Figure 35). The results of the flow model comparison are finally presented in the form of histograms showing the distribution of predicted and observed current speeds at the calibration sites (Figure 31 to Figure 35). For the purpose of sediment plume dispersion modelling it is important that the distribution of velocities be reproduced accurately since these will determine the erosion and deposition thresholds as well as the plume dispersion patterns and direction of residual movement. For sand transport modelling the representation of peak velocities is particularly important.

Figure 14 to Figure 20 show that both the amplitude and time of arrival of the tidal wave are well predicted by the flow model. The maximum differences are observed during the first half of the simulation at the locations where measured data were available (Gauges 1 to 4, Figure 17 to Figure 20). These differences are not observed in the comparison against published data (at Tapa Bay, Night Cliff and Darwin, Figure 14 to Figure 16), which suggests that they can be attributed to the use of tidal levels computed from tidal constituents, rather than measured tidal levels, for boundary conditions. While these differences in water surface level are relatively small, it is important to recognize that they could also be attributed to varying meteorological conditions, present in the observed data but not modelled. The small differences in the time of arrival of high water at Gauges 1 to 4 (Figure 17 to Figure 20) are well within the resolution of the flow model result output (15 minutes).

The quality of the model calibration-validation was assessed by calculating the difference in water surface levels between the model predictions and the measured values at each site. The results of this assessment are presented in Table 5 in terms of root mean square error (RMSE). The water levels at the calibration sites are predicted to within 0.26 m on average. The maximum differences are observed at the tide gauges nearest to the site. The root mean square error computed on the second half of the time record only (see above discussion) improves to about 0.20 m. It should be noted that these differences can be partly attributed to the small offset in time of arrival of the tidal wave. Still, the results presented below are considered very reasonable.

Table 5 Level differences between model predictions and measured values

	Locations (Figure 2 and Figure 6)						
	Darwin	Night Cliff	Tapa Bay	Gauge 1	Gauge 2	Gauge 3	Gauge 4
RMSE	0.26 m	0.26 m	0.23 m	0.28 m	0.27 m	0.27 m	0.28 m

Figure 22, Figure 24, Figure 26, Figure 28 and Figure 30 show that the direction of the currents predicted by the flow model is in very good agreement with the directions measured at most locations; generally well within 10°. The agreement is slightly less

satisfactory at Monitor 1 and Sentinel 2 (Figure 22 and Figure 28), but is still very reasonable. The peak current speeds predicted by the model are of the same order as those measured, although some discrepancies are apparent. Again the differences could be attributed to varying meteorological conditions in the observed values but not accounted for in the model. The analysis of predicted and measured current speeds in the 15-day cycle distributed in 5 cm/s bins, however, indicates that the proportion of time under a particular threshold is generally well reproduced by the flow model (Figure 31 to Figure 35). This is supported by the comparison of the tidal ellipses (same figures). The agreement is poorest at Sentinel 3 (Figure 35) but is still very reasonable.

The agreement between the model predictions and the measurements was quantified by calculating the average difference in current speeds. This difference was expressed in terms of root mean square error (RMSE, Table 6). The current speeds are predicted to within 0.21 m/s RMSE or better over the whole 15-day period. The maximum differences are observed on the western shores of Darwin Harbour approaches (Sentinel 2 and Sentinel 3). It may be relevant to note at this stage that the instrument set-up was different during these two deployments. Overall these results are considered acceptable.

Table 6 Speed differences between model predictions and measured values

Locations (Figure 4)					
	Monitor 1	Sentinel 1	Monitor 2	Sentinel 2	Sentinel 3
RMSE	0.10 m/s	0.13 m/s	0.10 m/s	0.21 m/s	0.19 m/s

These comparisons give confidence in the flow model predictions and their use to investigate the potential dispersion of sediment from the main subtidal areas of the East Arm where the dredging activities will take place.

A particular focus of the sediment plume dispersion modelling is to consider the potential for sediment accretion over the mangrove areas of Darwin Harbour. It is assumed that the elevation and friction of the mangroves determine both the amount of (turbid) water reaching the mangrove and the time water remains on those areas before the ebb. A detailed approach to representing this process was undertaken, so that it may be represented accurately, however, there remains a degree of uncertainty. Consequently sensitivity tests were undertaken; the sensitivity analysis to the friction factor used to represent the mangrove habitat is presented in Section 5.3.

4. Calibration-validation of the wave model

4.1 WAVE CALIBRATION PARAMETER

In TOMAWAC several physical processes can play a role in the calibration of the model, such as the choice of boundary conditions or the wave dissipation processes. In this study the waves in the East Arm are thought to be mainly the results of local wave growth due to wind. It was therefore considered appropriate to investigate the use of different white-capping formulations / dissipation coefficients as part of the wave model sensitivity testing and calibration. The default dissipation and weighting factors for the white-capping formulation (as specified in WAM-CYCLE4) were eventually retained.

4.2 SELECTED EVENTS

The wave model of Darwin Harbour was initially validated before being applied to predict the average and infrequently occurring wave conditions in the East Arm. This validation was carried out using wave data for a storm event with relatively high wave activity and noticeable wave-current interaction:

- February 8th 2009.

It is important that the wave model be able to predict accurately the tidal modulations (i.e. the increase or reduction in wave height depending on the current conditions) throughout a tidal cycle. If it can be shown that the model results agree with the in-situ measurements, then it gives greater confidence in the predicted wave conditions.

For the calibration-validation, significant wave heights and peak wave periods predicted by the wave model were compared against pressure transducer mooring data collected by *BMT WBM Pty Ltd.* (BMT) at two sites in the area of interest (Ref. 6). The locations of these points (PS02 and PS03) are marked by filled circles in Figure 2; their coordinates are given in Table 7. The instruments were deployed in approximately 13 m and 10 m water depth respectively. At this depth, the pressure signal from surface waves is attenuated, particularly from the short period waves. To some extent, this has been corrected for by BMT in their analysis of the data by applying appropriate frequency response functions.

Table 7 Locations where wave observations are available (see Figure 2)

	MGA Zone 52 Coordinates	
	(E)	(N)
PS02	689933.2	8632892.0
PS03	709598.6	8616335.0

The first pressure transducer mooring (PS03) was deployed in Darwin Harbour, directly north-west of Blaydin Point, on January 31st, 2009 and recovered on April 2nd, 2009. The other pressure transducer mooring (PS02) was installed out in the Beagle Gulf, in the approaches to Darwin Harbour, between February 1st, 2009 and April 3rd, 2009. There were no interruptions in the records at these locations. The wave data were collected every 12 minutes. The measured wave characteristics include significant wave height and peak wave periods. There is, however, no record of wave direction.

These records indicate that there is only a limited amount of wave energy entering the harbour from the Beagle Gulf, even when wave activity is high in the approaches to Darwin Harbour. Most of the wave activity at location PS03 is generated by wind locally within the Darwin Harbour, yielding short period waves of limited height at the dredging site.

Concurrent water level and velocity fields predicted by the calibrated flow model were included in all the wave model simulations. In addition, equivalent winds were applied over the wave model area to represent local wave generation due to winds. This may be particularly relevant for winds blowing from the north and north-east for example, which are characterised by longer fetches.

4.3 WAVE MODEL RESULT COMPARISON

The wave model was validated by comparing predicted significant wave heights and peak wave periods against the observed wave data surveyed by BMT in February 2009. The locations of the validation sites are marked by filled circles in Figure 2 and their coordinates have been reported in Section 4.2. The wave model was run at three-hourly intervals for the selected period of the validation data using water level and flow fields predicted by the flow model for the same periods.

The time series of significant wave height and absolute peak period are presented in Figure 36 and Figure 37 respectively. In these figures the wave model predictions are shown as symbols, while the measured data are shown as continuous lines.

Figure 36 and Figure 37 show that the predicted significant wave heights and peak wave periods agree reasonably with the measured conditions, although Figure 36 shows a tendency for the model to under-predict the wave heights in the approaches to Darwin Harbour (PS02). These differences could be a result of the assumptions made in the wave model. In particular the model was run to a steady-state from three-hourly boundary conditions. Also, the wind field used in these simulations was constant and did not vary spatially. Nonetheless, the wave heights at the site of interest (PS03) are quite limited (often below 0.3 m) and are generally well reproduced by the wave model.

5. *Application of the flow model*

The dispersion of material released either during the extraction or placement phases of the dredge cycle is primarily governed by the prevailing hydrodynamics. An effective flow model is paramount to the accurate representation of the advection and diffusion of material released into the water column. The approach chosen here is to determine appropriate driving conditions that will lead to a representation of typical sediment transport conditions, while maintaining acceptable simulation times.

5.1 BOUNDARY CONDITIONS FOR THE FLOW MODEL

In this study, time-varying water levels were applied along the offshore boundaries of the flow model. They were derived from data obtained from the C-Map database along the eastern model boundary and from the Mike-21 global model along the western model boundary (see Section 2.5).

A time record of published predicted water surface elevations (Ref. 3) was obtained for Darwin, for a 20-year period spanning from 1992 to 2011 inclusive. This record was analysed to identify the high and low waters and consequently the spring and neap cycles. The method described in Table V of the Admiralty Tide Tables (Ref. 7) was used to calculate HWS (High Water Spring), LWS (Low Water Spring), HWN (High Water Neap) and LWN (Low Water Neap) from the published data, i.e. the height of HWS was computed as the "average of the heights of two successive high waters during the period when the range of the tide is greatest", and the height of LWS was computed as the "average height obtained by the two successive low waters during the same period". The same approach was used for the neap tides. Once all the high and low waters were determined for spring and neap cycles and for the 20-year period, the average values were computed.

The same time record at Darwin was subsequently scanned to find a suitable period when average spring and average neap conditions occurred within approximately 7 days of each other. The resulting period representative of 20-year average conditions is April 23rd to May 7th, 2005. Although the target tidal ranges (spring and neap) were met exactly at Darwin, near the site of interest; the levels were marginally higher (within 10 cm) than the target levels.

It is implicitly assumed in this analysis that average conditions for the tidal range also correspond to average conditions for the tidal current, which is appropriate for tidal flows.

Table 8 puts the 20-year average conditions in context with respect to HAT (Highest Astronomical Tide) and LAT (Lowest Astronomical Tide).

Table 8 Spring and neap tidal ranges, HAT and LAT at Darwin

	Spring tidal range (m)	Neap tidal range (m)
20-year average	5.74	1.95
20-year low	4.08	0.67
20-year high	7.09	3.78

	(m MSL)	(m MSL)
HAT	3.93	
LAT		-4.17
Model levels	3.26	-3.84

(from simulation period)

5.2 METEOROLOGICAL CONDITIONS

In addition to tidal forcing the flow model was driven by winds. Experience and best judgment were used to derive wind conditions representative of most frequent and extreme conditions for the wet season (approximately October to March) and for the dry season (approximately April to September). Most frequent conditions were taken as 90th-percentile conditions, while ‘extreme’ conditions were taken as conditions with a 1-year return period. In the absence of long-term site-specific wind data, these were computed from the wind record at the NOAA Data Point by count-back analysis. Figure 11 and Figure 12 present seasonal wind climates (wind speed against wind direction) for the wet and dry seasons respectively.

The wind conditions applied in the flow model are summarized below in Table 9:

Table 9 Wind conditions applied in the model

		Wind speed (m/s)	Wind direction (°N)
dry	most frequent	9.3	120
	extreme E	13.8	90
wet	most frequent	9.0	270
	extreme W	17.4	270
	extreme NE	18.8	45

The winds were blown over the entire model area (spatially and temporally constant wind field).

Even though best judgement was applied to derive wind conditions representative of most frequent and extreme conditions, there remains some degree of uncertainty. A sensitivity analysis to the meteorological conditions used in the numerical model was therefore conducted. This analysis is presented in Section 5.4.

5.3 SENSITIVITY ANALYSIS: MANGROVE FRICTION COEFFICIENTS

As noted previously, a particular focus of the sediment plume dispersion modelling is to consider the potential for sediment accretion over the mangrove areas of Darwin Harbour. The numerical model area therefore includes the mangroves, as identified from geo-referenced contour data supplied by INPEX (Ref. 2). The analysis of these data

yielded a map of spatially-varying friction coefficients, dependent on the types of vegetation found in the mangrove, their density and strength (Appendix 2).

Best judgment was used to derive sensible friction coefficients based on the existing literature. The resulting coefficients are within appropriate physical ranges, but there remains some degree of uncertainty and a sensitivity analysis was conducted to investigate the impact of the mangrove friction coefficient on levels and velocities in the main channels of Darwin Harbour.

For that purpose the model results using the finely resolved friction map (Appendix 2) were compared to model results using a constant friction coefficient over the mangroves (same values in the main body of water; a constant Chézy value of 30, which is typical of rough seabed, over the mangrove areas).

The average differences in water surface levels and current speeds were computed at a range of locations within Darwin Harbour and expressed in terms of root mean square difference (Table 10). It resulted that the current speeds were within 0.01 m/s or less over the whole 15-day period; similarly the water levels were within 0.01 m or less.

Table 10 Effect of the friction coefficient in the mangroves on levels and speeds

	Locations (Figure 4)				
	Monitor 1	Sentinel 1	Monitor 2	Sentinel 2	Sentinel 3
RMSE Levels	0.01 m	0.01 m	-	-	-
RMSE Velocities	-	0.01 m/s	0.01 m/s	0.01 m/s	0.01 m/s

This analysis therefore indicates that the hydrodynamics in Darwin Harbour are relatively insensitive to the representation of the mangroves in the model. Although it was not possible to calibrate the flow model in these areas, the analysis presented in Appendix 2 is thorough and deemed appropriate for this study.

5.4 SENSITIVITY ANALYSIS: METEOROLOGICAL CONDITIONS

The flow model results drive in part the sediment plume dispersion model. The difficulty is to determine appropriate driving conditions that will lead to a representation of typical sediment transport conditions. The approach chosen in this study was to combine a 20-year average spring-neap tidal cycle with typical to “extreme” wind conditions. These conditions are summarised in Table 8 and in Table 9.

A sensitivity analysis was conducted to investigate the impact of the meteorological conditions on levels and velocities in Darwin Harbour. The results of this analysis are presented in Table 11. They are expressed in terms of root mean square differences (RMSE) with reference to the simulation with average tidal conditions but no wind, and at the sites where the flow model have been calibrated. It is clear from Table 11 that typical (most frequent) wind conditions have a very limited impact on both water levels and velocities. For more extreme conditions (return period of a year), the current speeds were predicted within 0.17 m/s or less of the base conditions over the whole 15-day period; the water levels were predicted within 0.29 m or less of the base conditions.

Table 11 Effect of meteorological conditions on levels and speeds

		Locations (Figure 4)				
Wind conditions		Monitor 1	Sentinel 1	Monitor 2	Sentinel 2	Sentinel 3
RMSE Levels	dry season – most frequent	0.04 m	0.05 m	0.04 m	0.04 m	0.04 m
	dry season – extreme E	0.12 m	0.14 m	0.11 m	0.11 m	0.10 m
	wet season – most frequent	0.03 m	0.04 m	0.03 m	0.03 m	0.03 m
	wet season – extreme W	0.25 m	0.29 m	0.24 m	0.23 m	0.22 m
	wet season – extreme NE	0.12 m	0.13 m	0.11 m	0.12 m	0.11 m
RMSE Velocities	dry season – most frequent	0.04 m/s	0.03 m/s	0.02 m/s	0.02 m/s	0.03 m/s
	dry season – extreme E	0.08 m/s	0.06 m/s	0.05 m/s	0.05 m/s	0.09 m/s
	wet season – most frequent	0.03 m/s	0.02 m/s	0.01 m/s	0.01 m/s	0.03 m/s
	wet season – extreme W	0.08 m/s	0.09 m/s	0.07 m/s	0.07 m/s	0.15 m/s
	wet season – extreme NE	0.08 m/s	0.06 m/s	0.10 m/s	0.08 m/s	0.17 m/s

The effect of the meteorological conditions was also quantified in terms of surge component (change to the mean sea level within Darwin Harbour) (Table 12). The dry season, which is characterised by winds predominantly from the E to ESE (Figure 12), leads to negative surge components at all the sites considered in this analysis. The wet season, which is characterised by winds predominantly from the WSW to WNW (Figure 11), yields positive surge components of up to 0.25 m for westerly wind conditions. There is no noticeable change in the water level for north-easterly winds during the wet season.

Table 12 Surge as a result of meteorological conditions

	Surge (m)				
	Most frequent dry (120°N)	Extreme dry (90°N)	Most frequent wet (270°N)	Extreme wet (270°N)	Extreme wet (45°N)
Monitor 1	-0.04	-0.10	0.03	0.22	0.00
Sentinel 1	-0.04	-0.12	0.03	0.25	-0.02
Monitor 2	-0.04	-0.09	0.03	0.20	-0.01
Sentinel 2	-0.04	-0.09	0.03	0.21	0.01
Sentinel 3	-0.03	-0.09	0.02	0.19	0.00

6. *Conclusions*

The dispersion of material released either during the extraction or placement phases of the dredge cycle is primarily governed by the prevailing hydrodynamics. An effective flow model is paramount to the accurate representation of the advection and diffusion of material released into the water column.

The comparisons of the flow model results against both time histories of water surface elevations and observed current data give confidence in the flow model predictions and their use to investigate the potential dispersion of sediment from the main subtidal areas of the East Arm where the dredging activities will take place. The comparisons of the wave model results against observed wave data indicate that the model tends to under-predict the wave heights in the approaches to Darwin Harbour, but it generally reproduces them well at the dredging site. It may be important to remember that wave activity is naturally limited in the East Arm.

Additional analyses were performed to determine the sensitivity of the flow model results to the mangrove friction coefficients and to the meteorological conditions. These analyses indicated that the hydrodynamics in Darwin Harbour are relatively insensitive to the physical representation of the vegetation in the model, although the tidal volume it covers is critical. They also showed that typical wind conditions have a very limited impact on both water levels and velocities. Their impact is more pronounced for more extreme conditions. The effect of the meteorological conditions was also quantified in terms of surge component. The assumptions made in this study are therefore deemed appropriate.

7. *References*

- Ref. 1. NOAA WAVEWATCH III™ global wave model data
(<ftp://polar.ncep.noaa.gov/pub/history/waves/>)
- Ref. 2. Geo-referenced contour data of the mangrove, INPEX
inpe_x_gis_GISADMIN_ENVR_NTY_NtGovtData_NRT_20080221_M52_MangrovesDarwinHarbour25k.shp
August 2009.
- Ref. 3. Hourly sea level and meteorological data at Darwin, Australian Baseline Sea Level Monitoring Project
(<http://www.bom.gov.au/oceanography/projects/abslmp/data/index.shtml>)
- Ref. 4. Fugro bathymetry dataset, obtained through INPEX
DarwinHarbourSurvey_Fugro.gdb
September 2009.
- Ref. 5. MIKE C-MAP, Version 9.0.1020 and C-Map's 93.3 database. Copyright © 2002 DHI Water & Environment. Copyright © 2002 C-Map Norway.
- Ref. 6. BMT WBM Pty Ltd. “Metocean Data Collection in Darwin Harbour” Report No R.B17183.001.00. May 2009.
- Ref. 7. “Admiralty Tide Tables. Pacific Ocean, Volume 4” The United Kingdom Hydrographic Office. 2009.

Glossary

<i>Term</i>	<i>Definition</i>
90 th -percentile	The value in a set where 10% of values are greater, and 90% are lower.
95 th -percentile	The value in a set where 5% of values are greater, and 95% are lower.
accretion	The build-up of sediment on subtidal and intertidal zones; the opposite of erosion.
acoustic doppler current profiler (ADCP)	A scientific instrument which transmits pulses of sound at a fixed frequency and, using the Doppler effect, can estimate the speed of the flow of water by measuring the frequency of the echoes returning from sound scatters in the water (such as small particles or plankton) that reflect the sound back to the ADCP.
advection	Refers to the transportation of a substance by the bulk movement of water (such as an ocean current).
bathymetry; bathymetric	Refers to the measured depths of a body of water, normally relative to LAT.
C-Map	A commercially available computer software package having marine navigation charts in electronic form, allowing display of one or more layers of information from one or more charts on a computer monitor. For numerical modelling work, the bathymetry data can be extracted in editable format. It is also able to produce time series tidal predictions for all primary and secondary ports listed in tide tables.
Chézy value	The coefficient used to compute the bed stress (force per unit area exerted by moving water on the bed (and vice versa) when using the Chézy friction law.
diffusion	The movement of particles of a substance from an area of higher concentration to an area of lower concentration due to molecular and turbulent motions.
Dredging Case Study	The dredging plan (i.e. equipment to be used and timing schedule) developed to minimise environmental impact by refining various methodologies relating to the dredging of the different components within the dredging footprint, and used as the basis for predictions of environmental impacts.
dredging footprint	The area of seabed delineated by the boundary between that part of the seabed to be disturbed by the dredging process and that part which will remain in its natural state.
HAT	Highest Astronomical Tide—the highest tide that can be expected to occur under average atmospheric conditions (i.e. calm wind; standard air pressure of 1016 millibars). More precisely, HAT is defined in Table V of the Admiralty Tide Tables (Ref. 7).
hydrodynamics	Refers to the characteristics of fluids in motion; the nature of the movement of fluids.
intertidal zone (or area)	The area of foreshore that is exposed to the air at low tide and underwater at high tide.

Term	Definition
JONSWAP spectrum	The JONSWAP (Joint North Sea Wave Project) spectrum is an empirical relationship that defines the distribution of energy with frequency within the ocean. In the JONSWAP spectrum, the wave spectrum is never fully developed and may continue to develop due to non-linear wave-wave interactions for a very long time. Therefore, in the JONSWAP spectrum, waves continue to grow with distance (or time), and the peak in the spectrum is generally quite pronounced.
LAT	Lowest Astronomical Tide—the lowest tide that can be expected to occur under average atmospheric conditions (i.e. calm wind; standard air pressure of 1016 millibars). It is used as the level from which water depths are measured. A negative value indicates a level below LAT. More precisely, LAT is defined in Table V of the Admiralty Tide Tables (Ref. 7).
Mike 21 global model	The MIKE 21 toolbox can be used to produce tidal predictions generated from global tidal model with harmonic constituents at $\frac{1}{4}$ or $\frac{1}{2}$ degree intervals. The constituents used are: M2, S2, K1, O1, N2, P1, K2, and Q1. The accuracy of the global model varies across different locations due to the coarse grid size and the interpolation methods used.
MHWN	The abbreviation for mean high water neaps—the long-term average water level reached at high tide during neap tides. More precisely, MHWN is defined in Table V of the Admiralty Tide Tables (Ref. 7).
MHWS	The abbreviation for mean high water springs—the long-term average water level reached at high tide during spring tides. More precisely, MHWS is defined in Table V of the Admiralty Tide Tables (Ref. 7).
MLWN	The abbreviation for mean low water neaps—the long-term average water level reached at low tide during neap tides. More precisely, MLWN is defined in Table V of the Admiralty Tide Tables (Ref. 7).
MLWS	The abbreviation for mean low water springs—the long-term average water level reached at low tide during spring tides. More precisely, MLWS is defined in Table V of the Admiralty Tide Tables (Ref. 7).
MSL	The abbreviation for mean sea level. More precisely, MSL is defined in Table V of the Admiralty Tide Tables (Ref. 7).
neap tide	A tide which has smaller than average range between low and high water; neap tide periods occur twice a month, when sun, earth and moon are furthest from being in line.
root mean square error (RMSE)	A measure of the differences between values predicted by a model and the values actually observed from the item being modelled. It is used as a measure of precision as it aggregates the individual differences (residuals) into a single measure of predictive power.
significant wave height (H_s)	The average wave height (trough to crest) of the largest one-third of waves passing a given point.
spring tide	A tide which has the larger than average range between low and high water; spring tide periods occur twice a month, when sun, earth and moon are closest to being in line.
subtidal zone (or area)	The zone in the ocean below the lowest water line (i.e. below LAT). It immediately adjoins the intertidal zone.

<i>Term</i>	<i>Definition</i>
TELEMAC-2D	A free-surface flow suite of solvers developed by a kernel of European organisations including the Laboratoire National d'Hydraulique et Environnement, Electricité de France, the Federal Waterways Engineering and Research Institute of Germany and HR Wallingford in the UK.
wave period (T_p)	An indication of the time interval (normally in seconds) for successive wave crests to pass a given point. Peak period refers to the time interval between the medium and larger wave crests, corresponding to the inverse of the frequency at which the wave energy spectrum would have its maximum value.

Figures

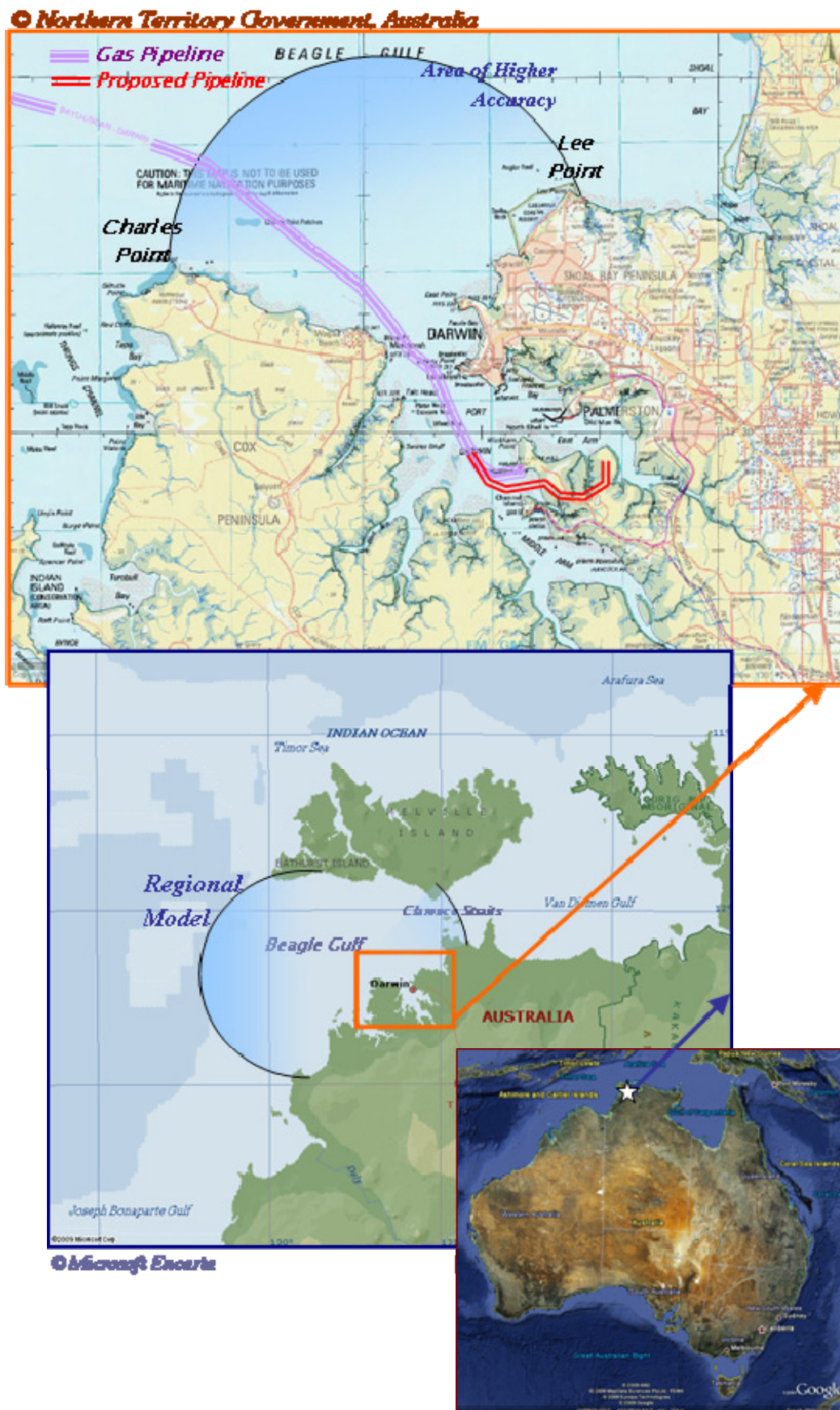


Figure 1 Geographic location of Darwin Harbour

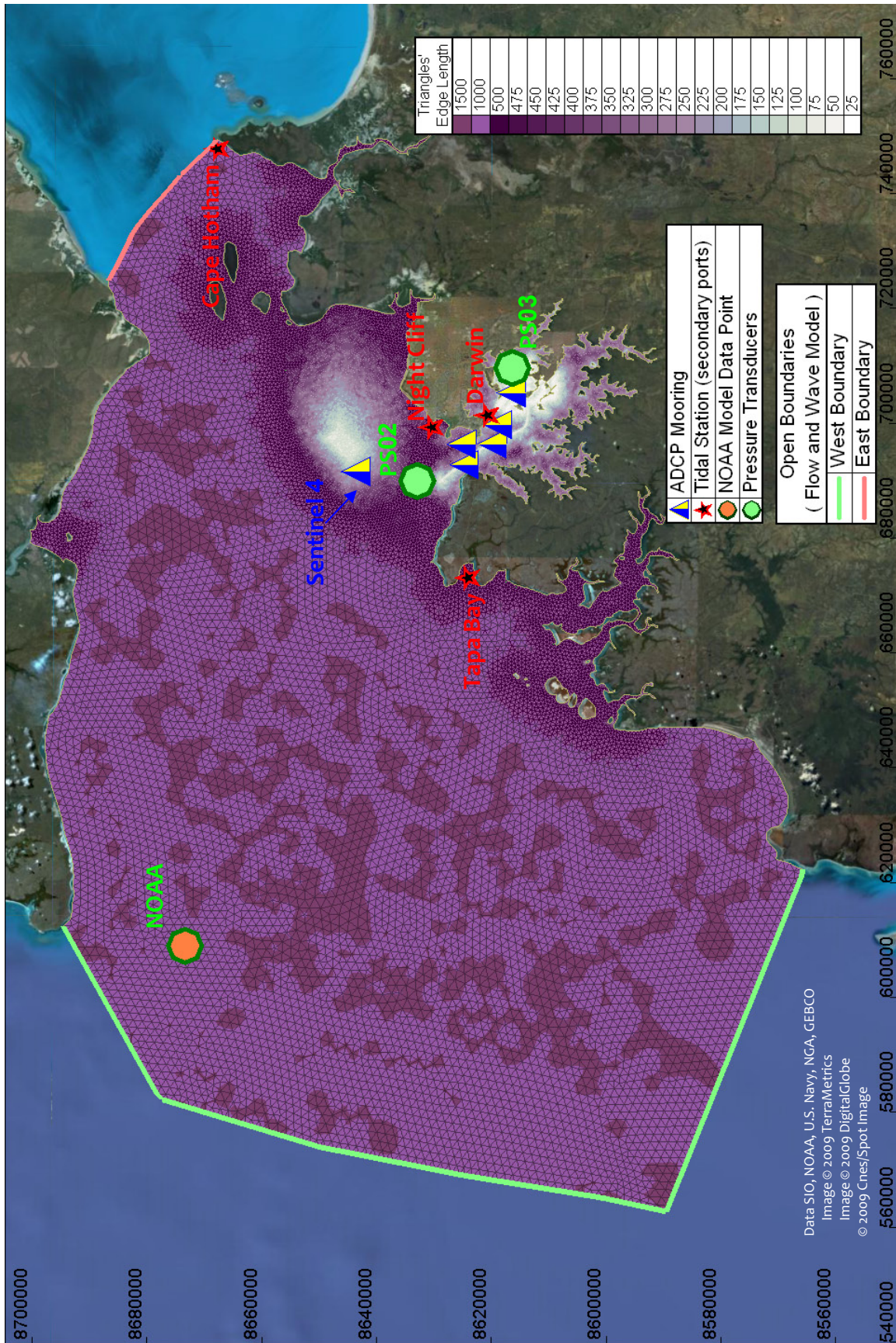


Figure 2 Model extent, mesh resolution and available datasets, View of Beagle Gulf

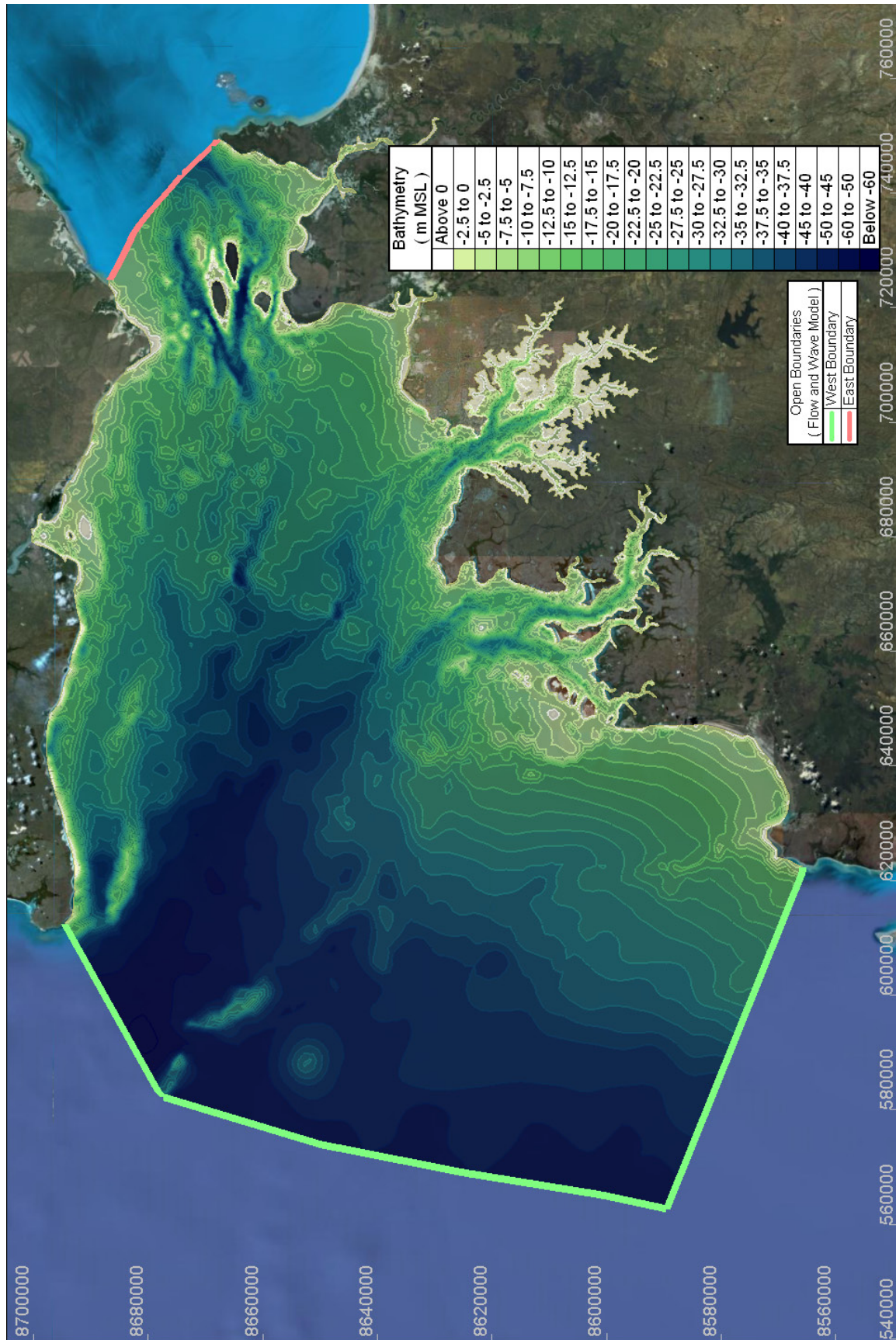


Figure 3 Bathymetry of the flow and wave models, View of Beagle Gulf

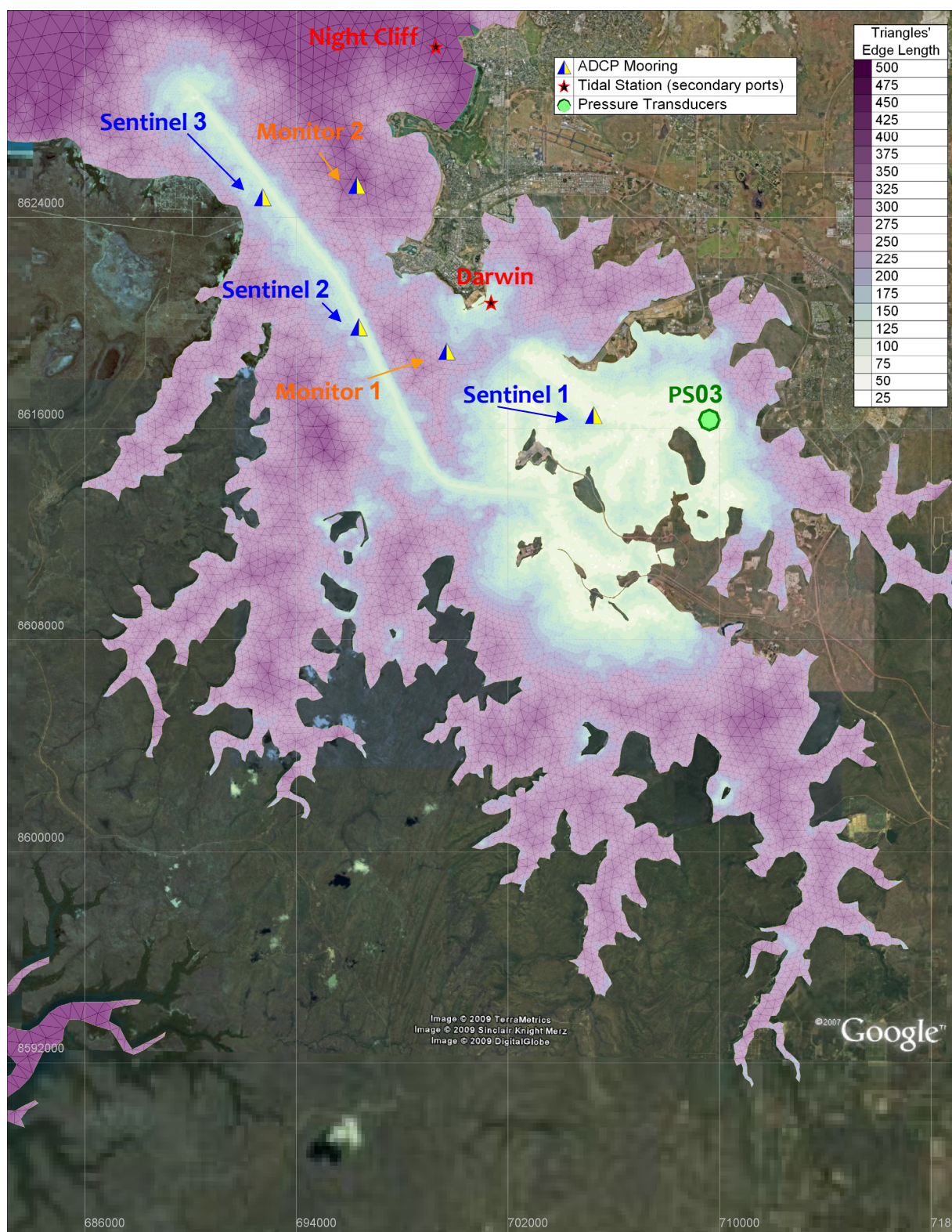


Figure 4 Numerical model mesh resolution and available datasets, Close-up view of Darwin Harbour

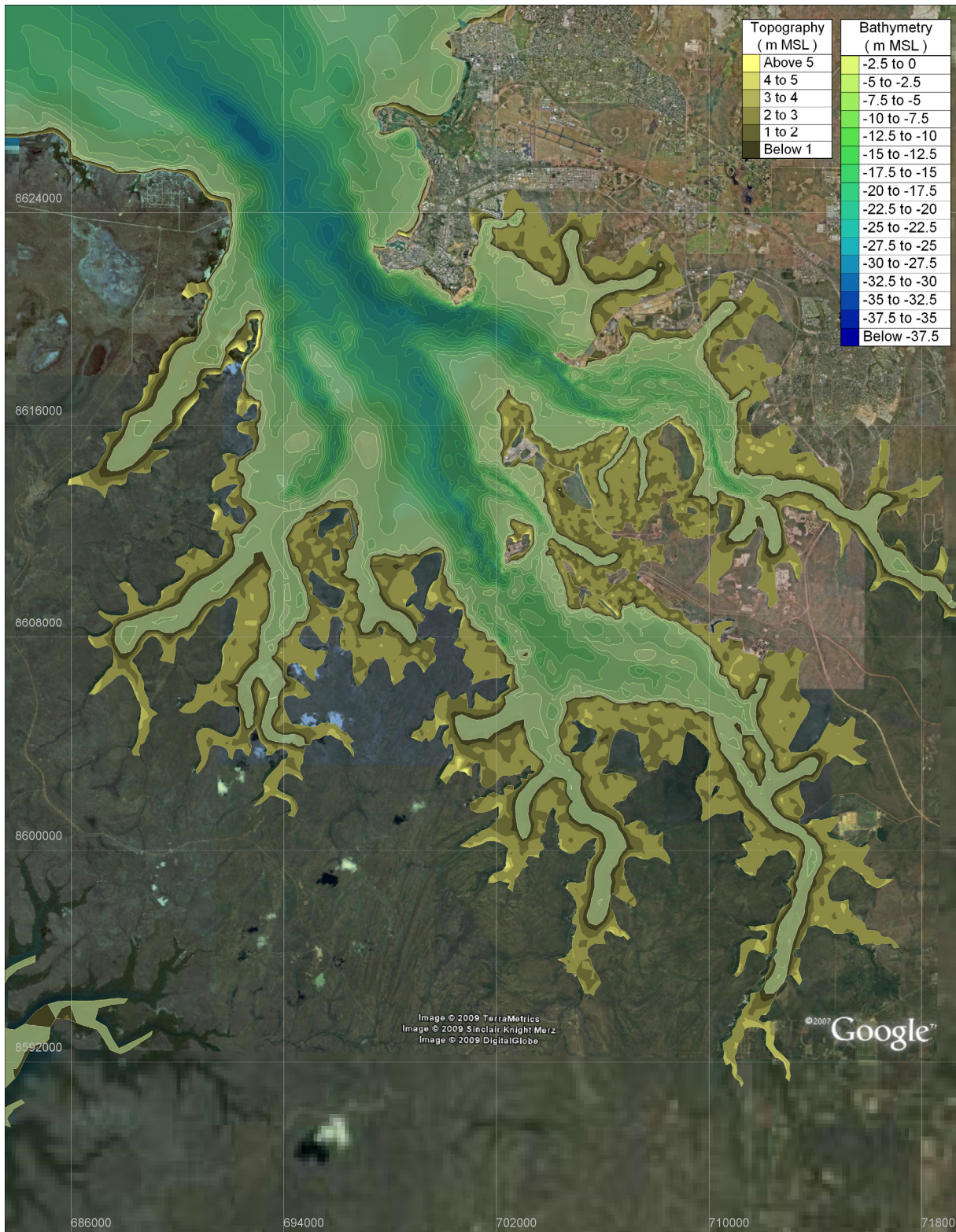


Figure 5 Bathymetry of the flow and wave models, Close-up view of Darwin Harbour

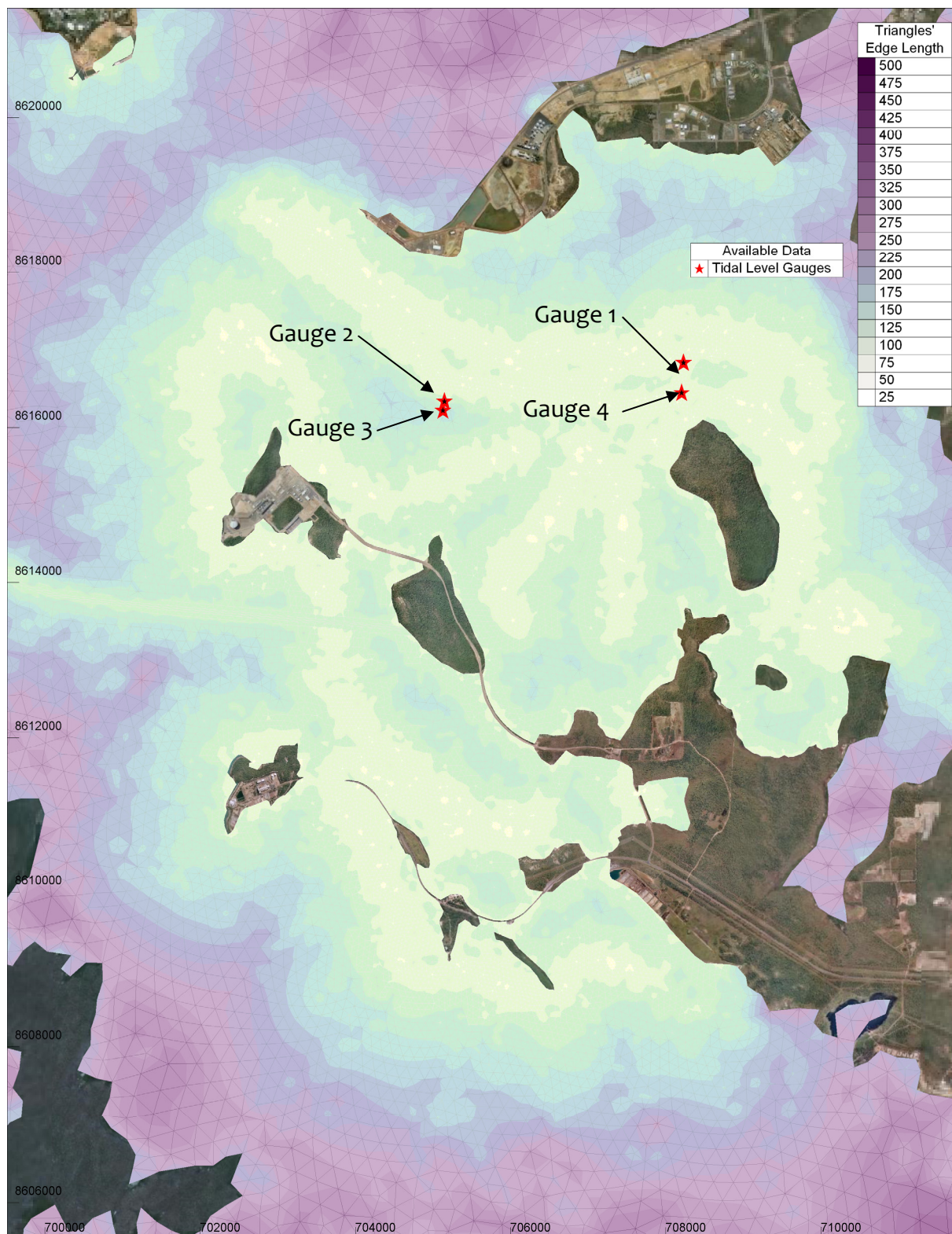


Figure 6 Model mesh resolution and available datasets, Close-up view of Blaydin Point

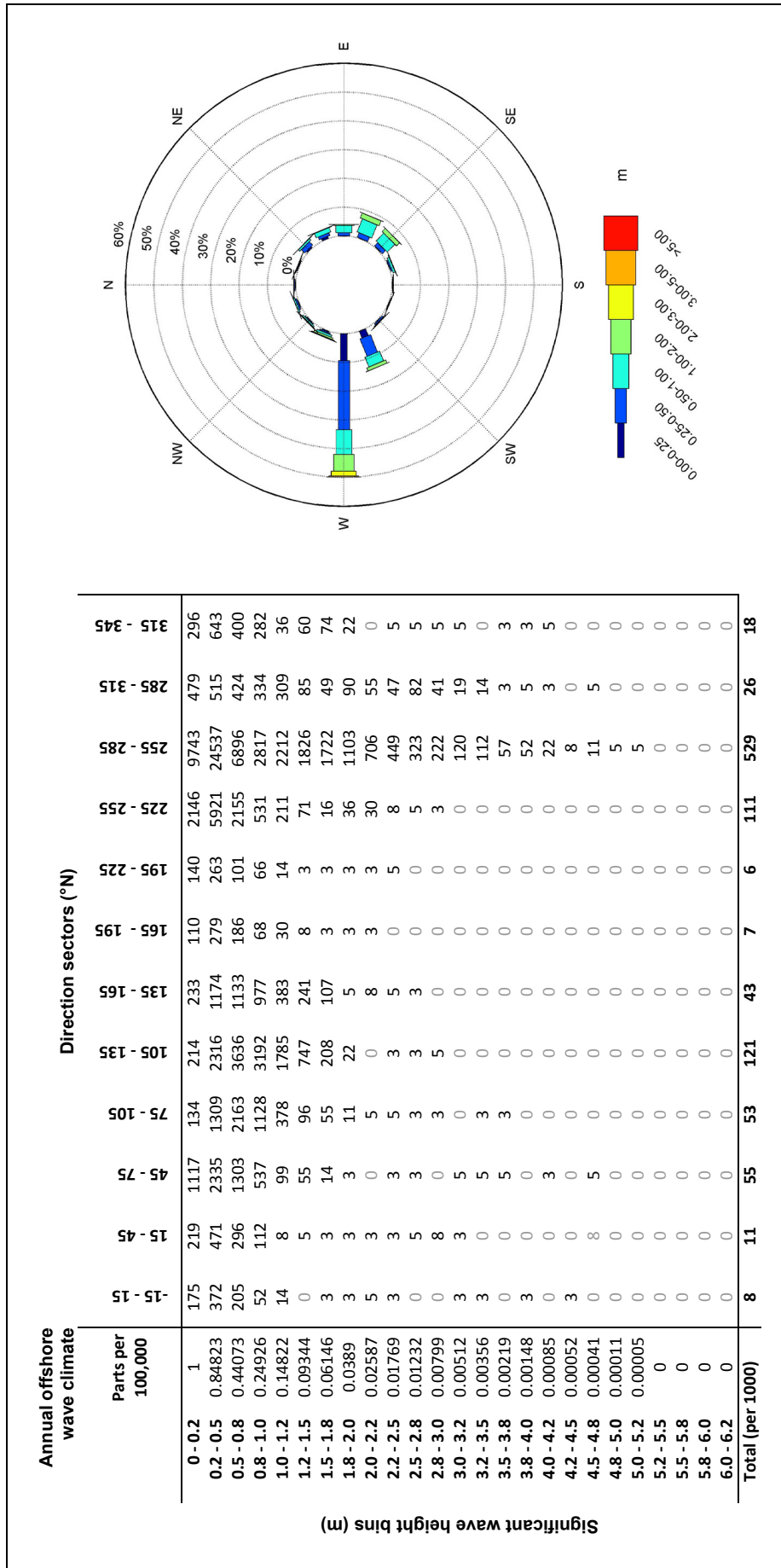


Figure 7 Annual offshore wave climate and wave rose, NOAA Data Point

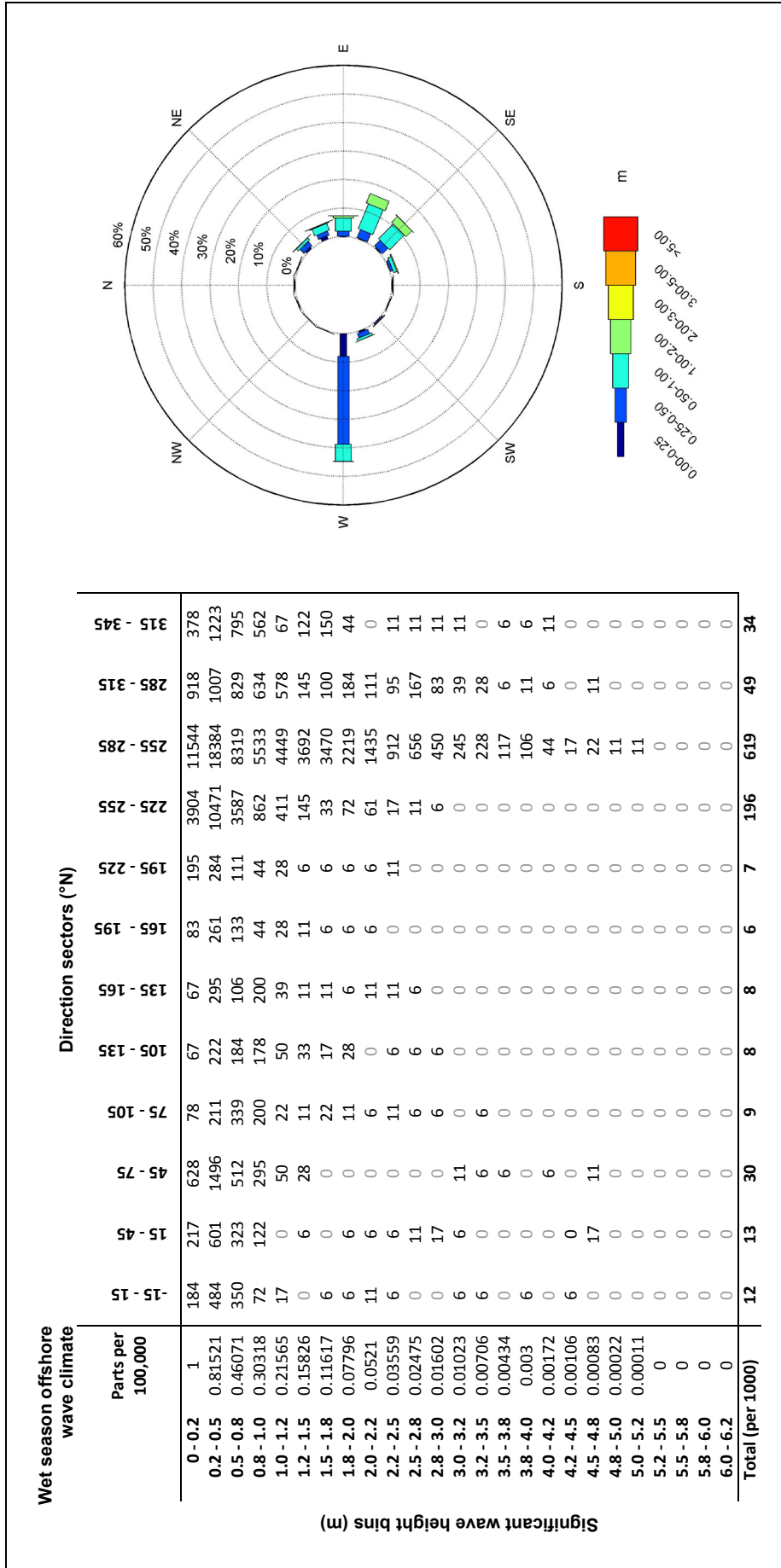


Figure 8 Wet season offshore wave climate and wave rose, NOAA Data Point

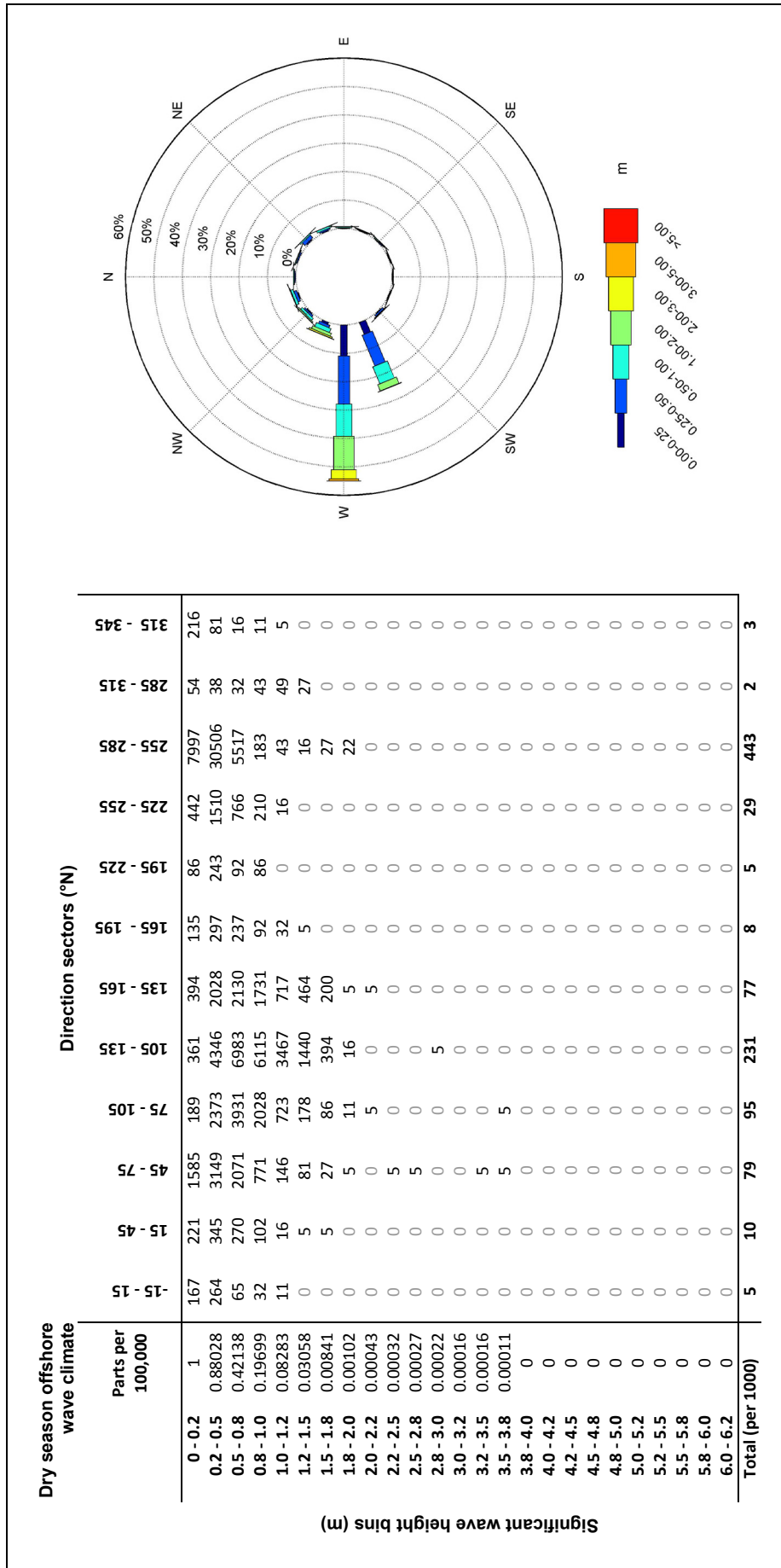


Figure 9 Dry season offshore wave climate and wave rose, NOAA Data Point

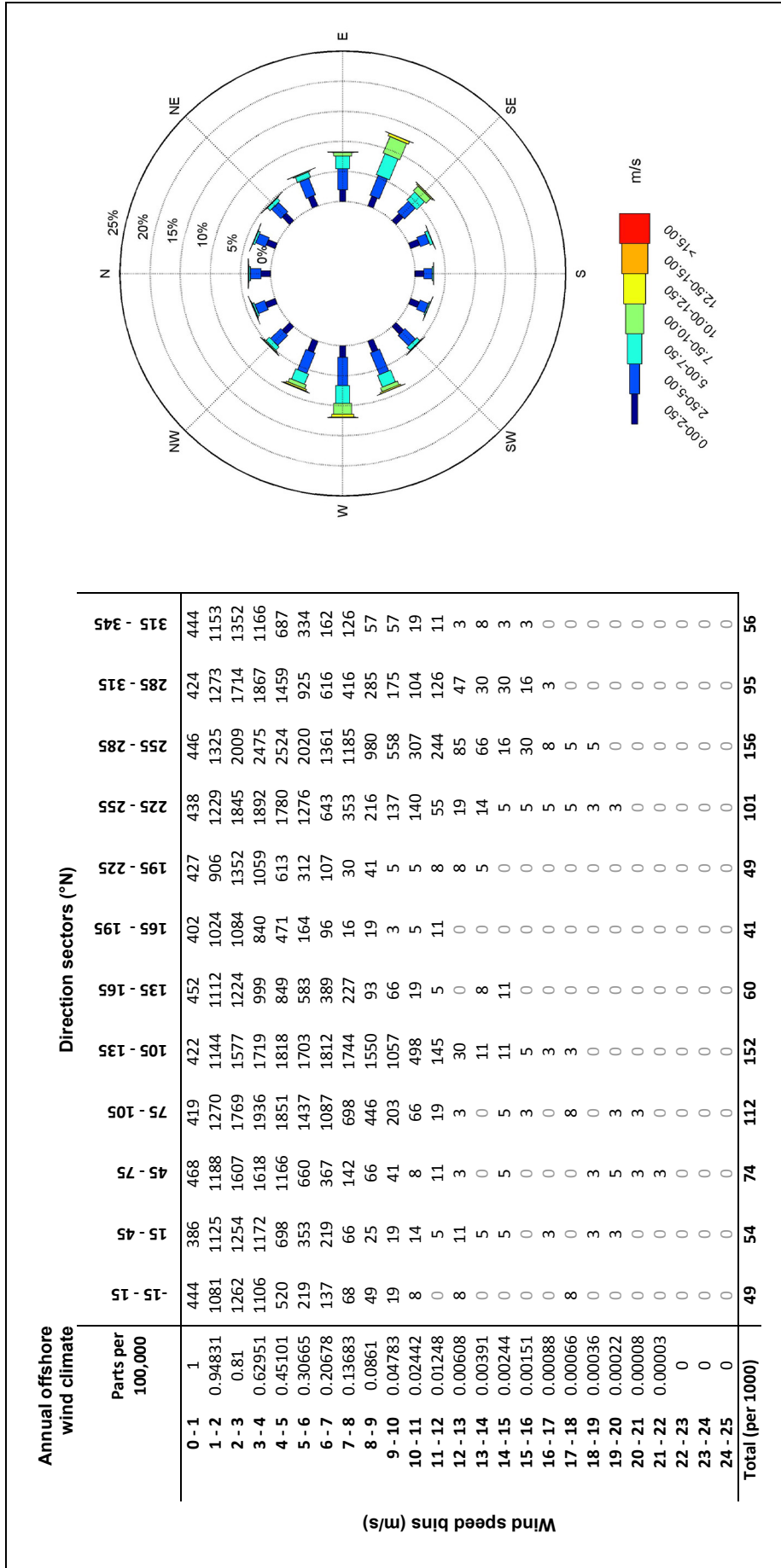


Figure 10 Annual offshore wind climate and wind rose, NOAA Data Point

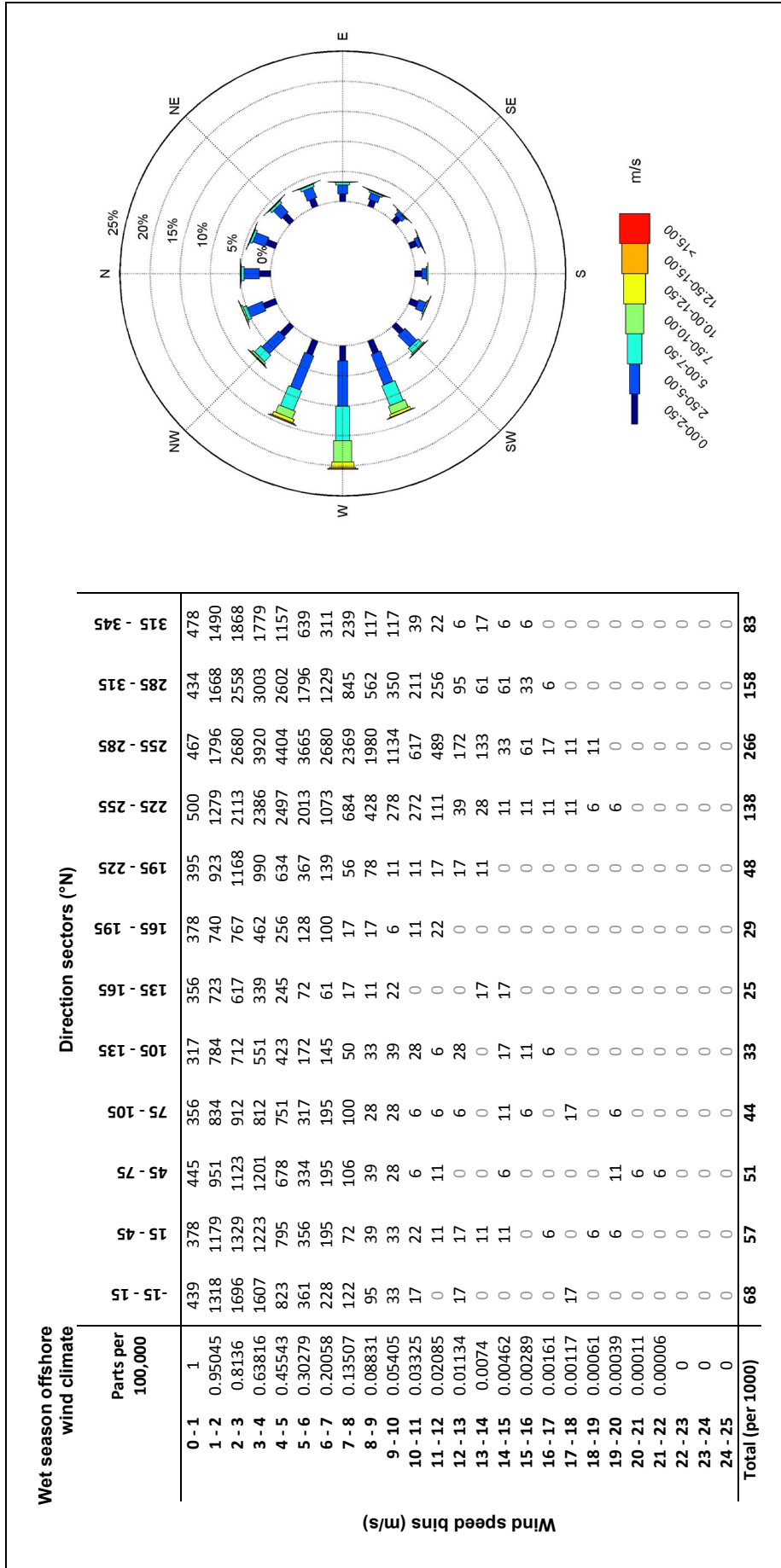


Figure 11 Wet season offshore wind climate and wind rose, NOAA Data Point

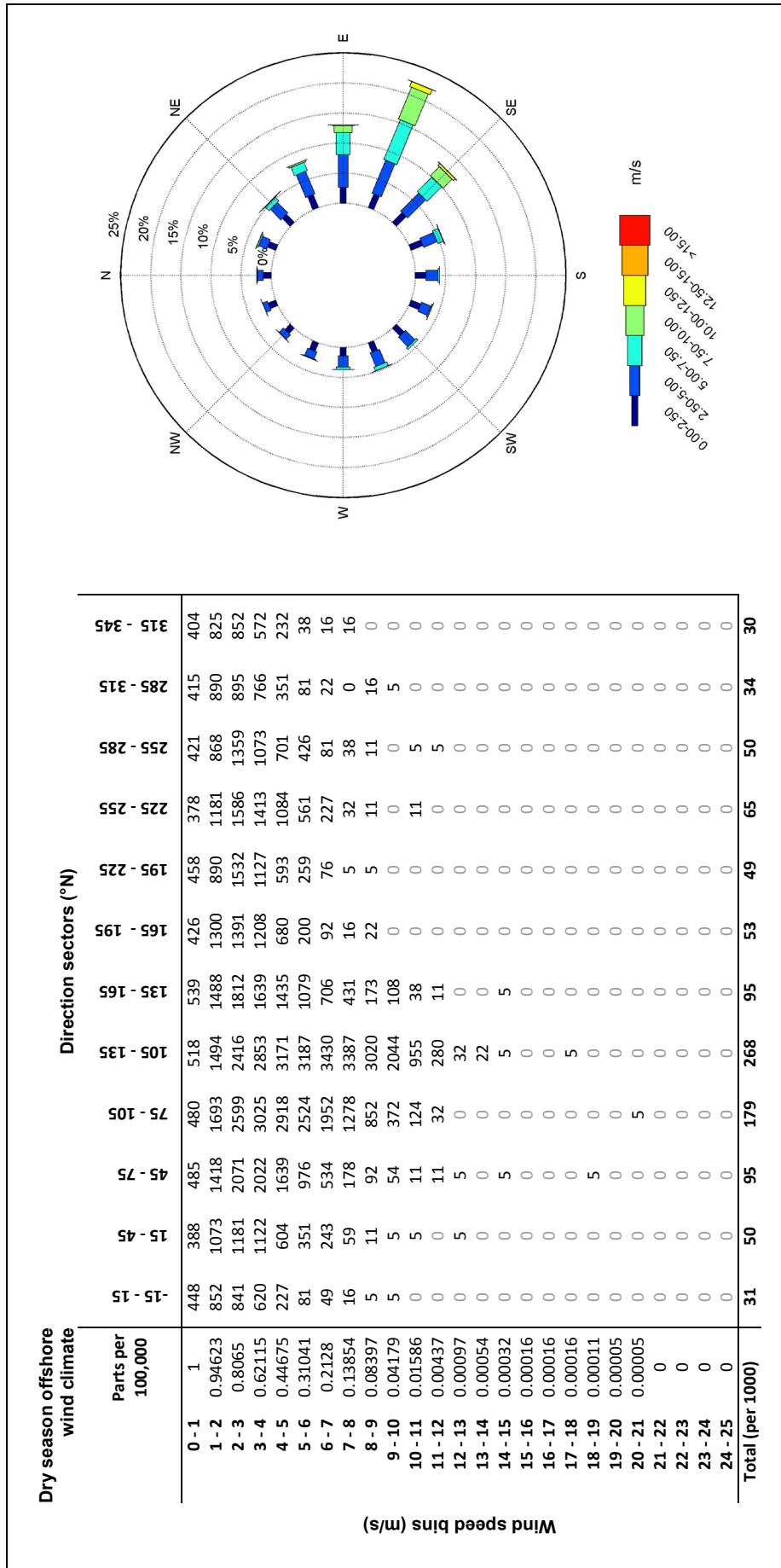


Figure 12 Dry season offshore wind climate and wind rose, NOAA Data Point

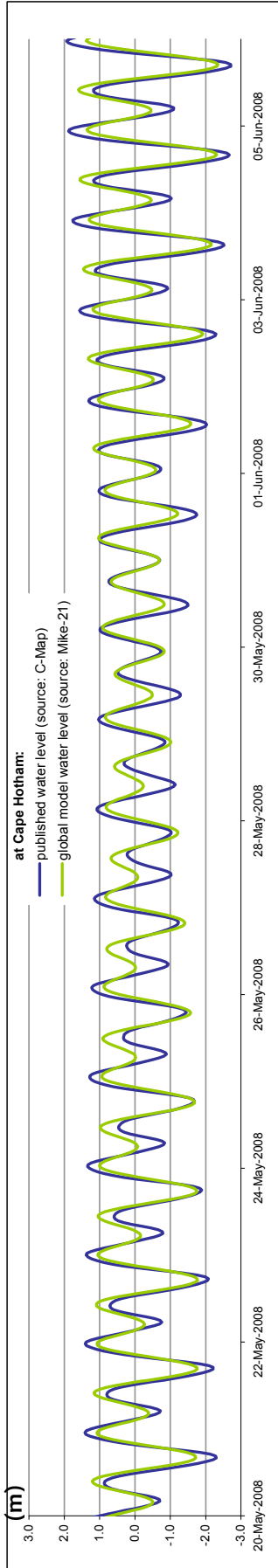


Figure 13 Water level at Cape Hotham, Differences in published data (Mike-21 / C-Map)

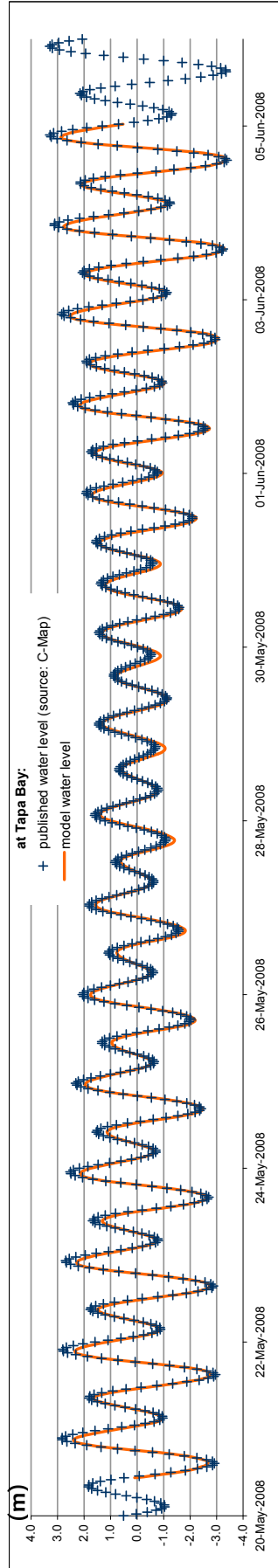


Figure 14 Water level at Tapa Bay, Model comparison against C-Map data

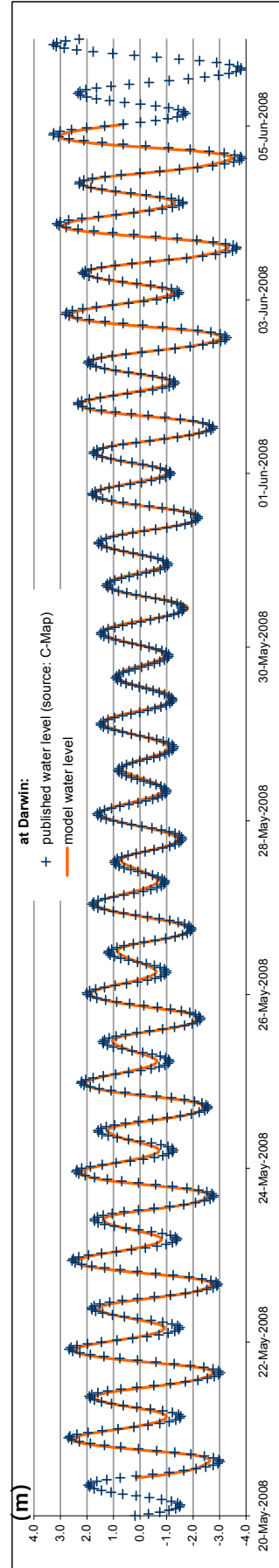


Figure 15 Water level at Darwin, Model comparison against C-Map data

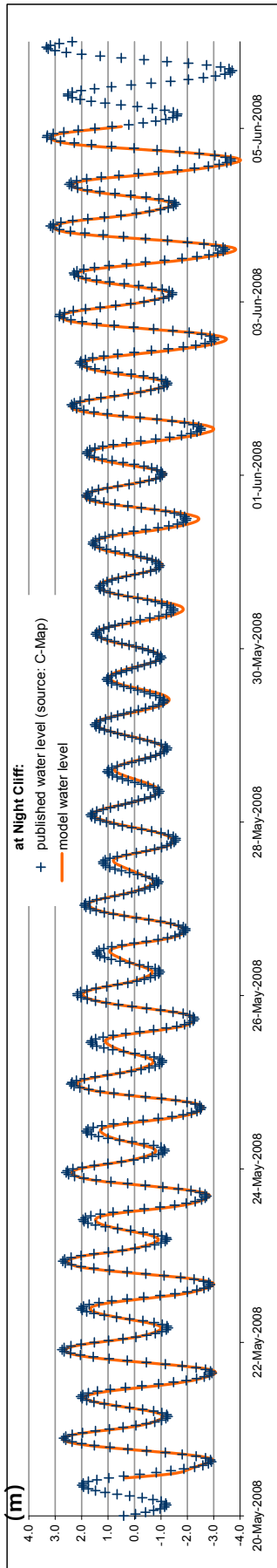


Figure 16 Water level at Night Cliff, Model comparison against C-Map data

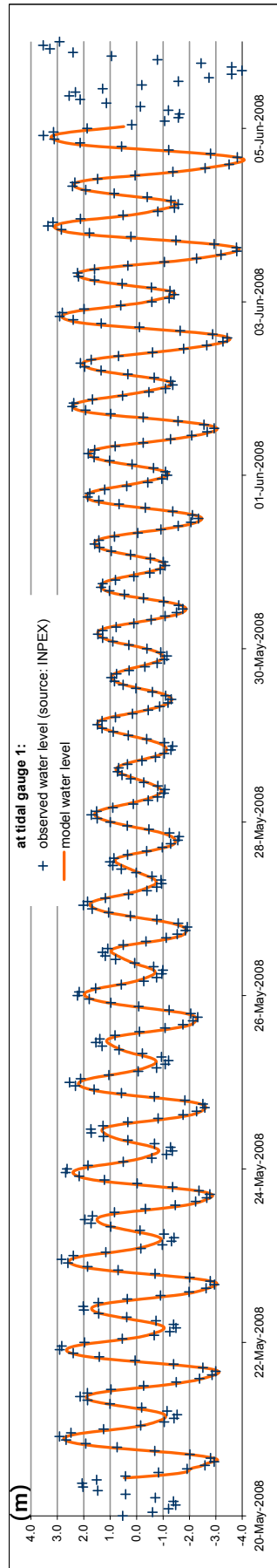


Figure 17 Water level at Gauge 1, Model comparison against observed data

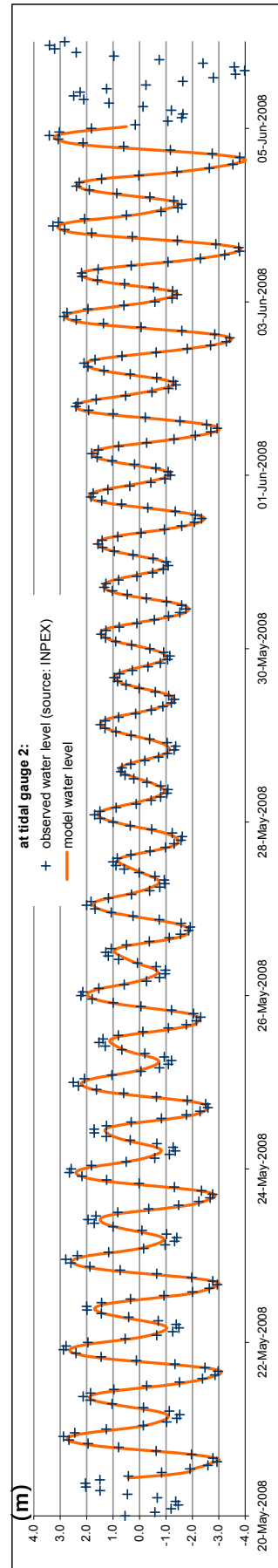


Figure 18 Water level at Gauge 2, Model comparison against observed data

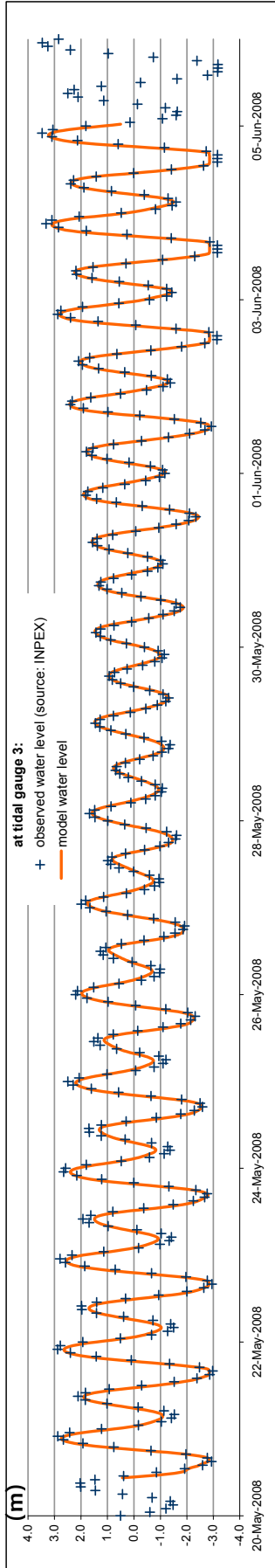


Figure 19 Water level at Gauge 3, Model comparison against observed data

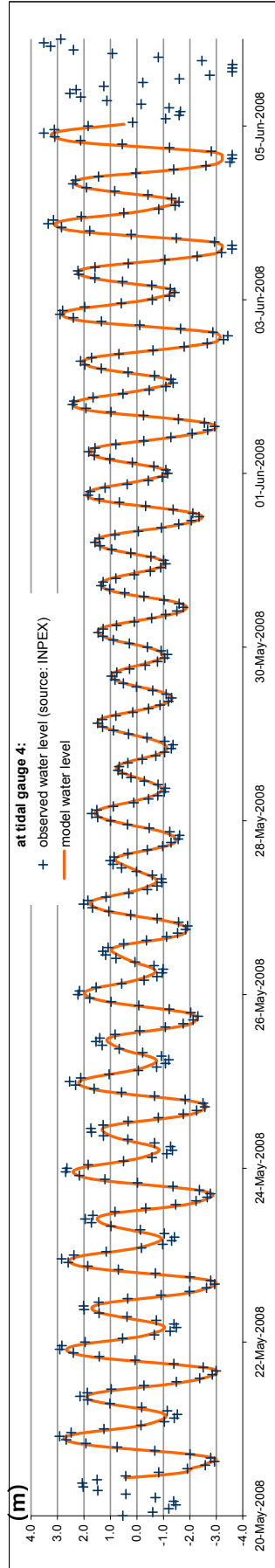


Figure 20 Water level at Gauge 4, Model comparison against observed data

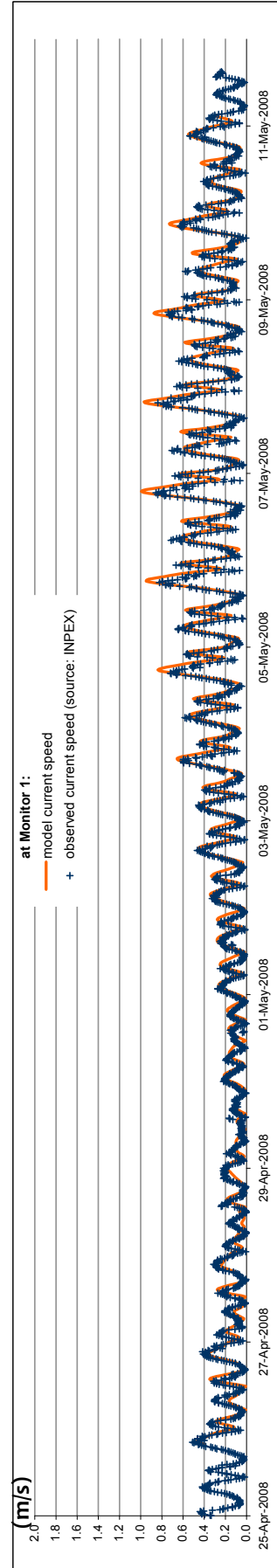


Figure 21 Current speed at Monitor 1, Model comparison against observed data

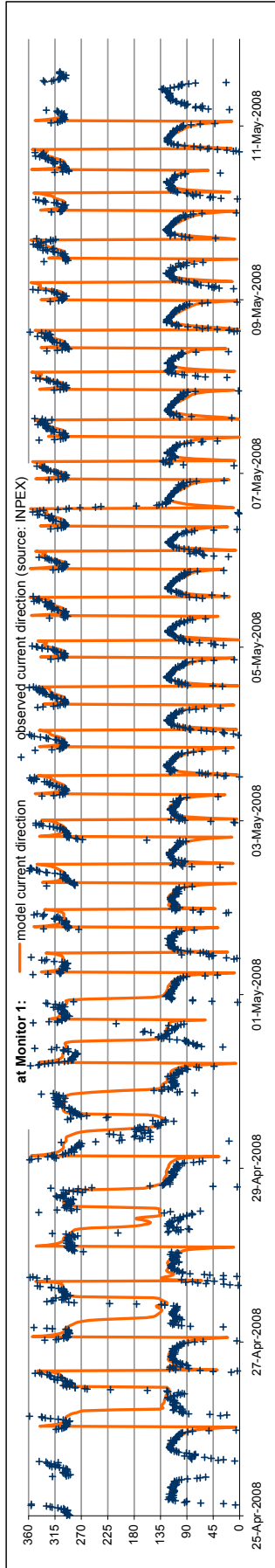


Figure 22 Current direction at Monitor 1, Model comparison against observed data

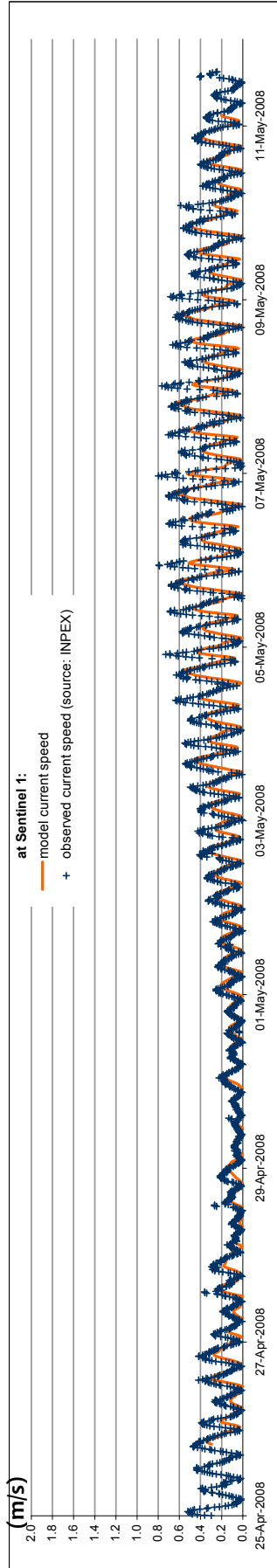


Figure 23 Current speed at Sentinel 1, Model comparison against observed data

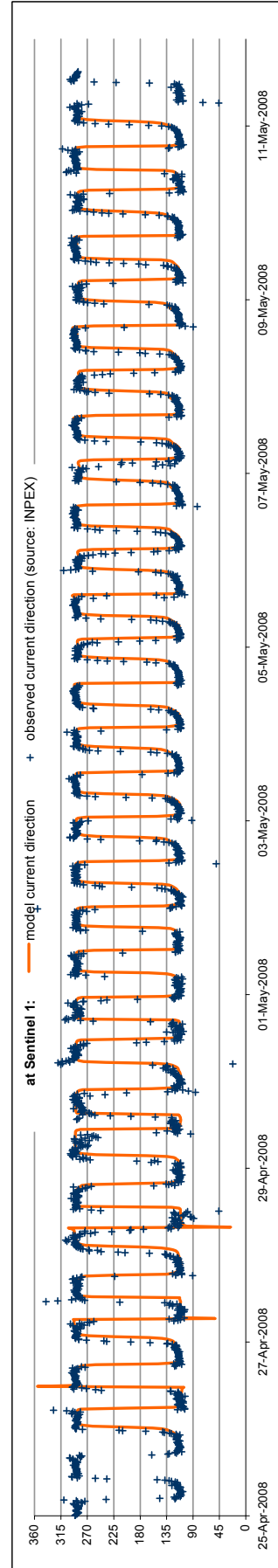


Figure 24 Current direction at Sentinel 1, Model comparison against observed data

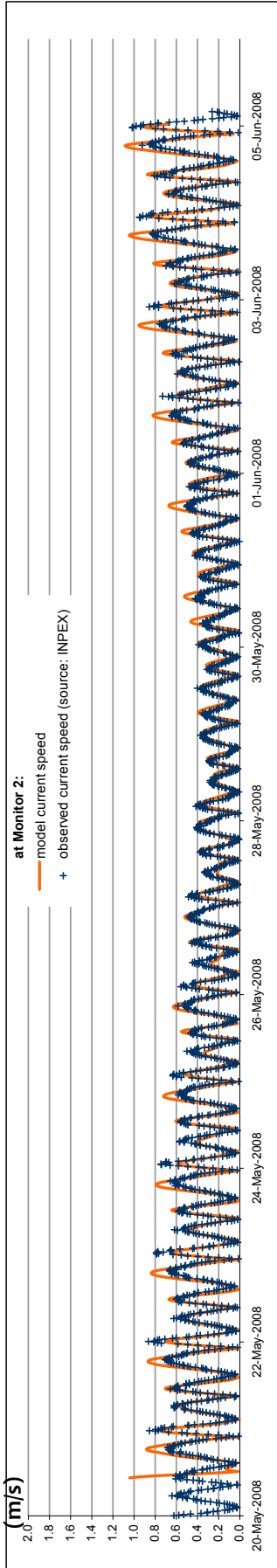


Figure 25 Current speed at Monitor 2, Model comparison against observed data

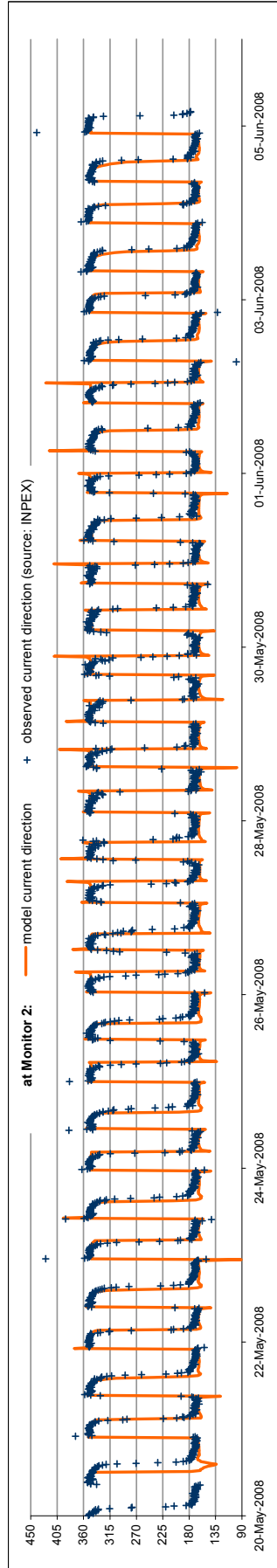


Figure 26 Current direction at Monitor 2, Model comparison against observed data

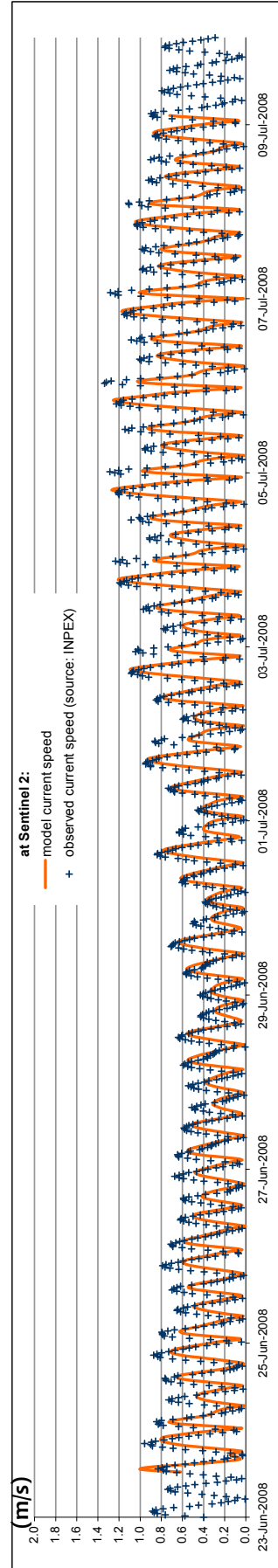


Figure 27 Current speed at Sentinel 2, Model comparison against observed data

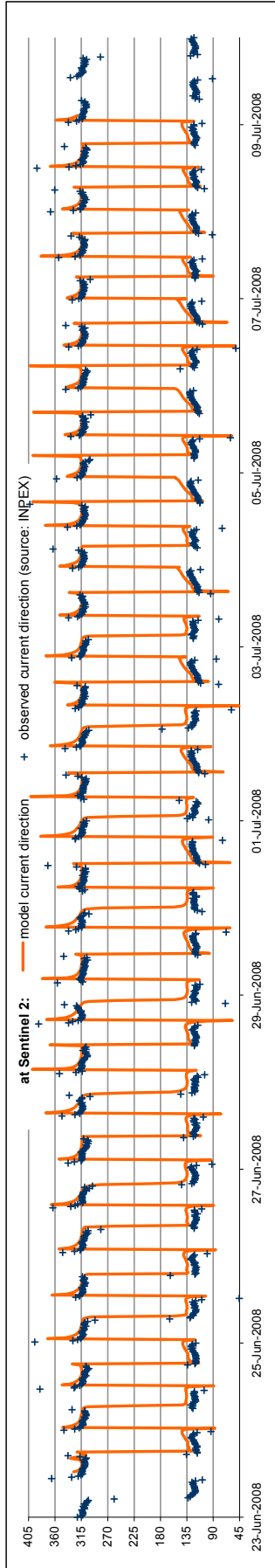


Figure 28 Current direction at Sentinel 2, Model comparison against observed data

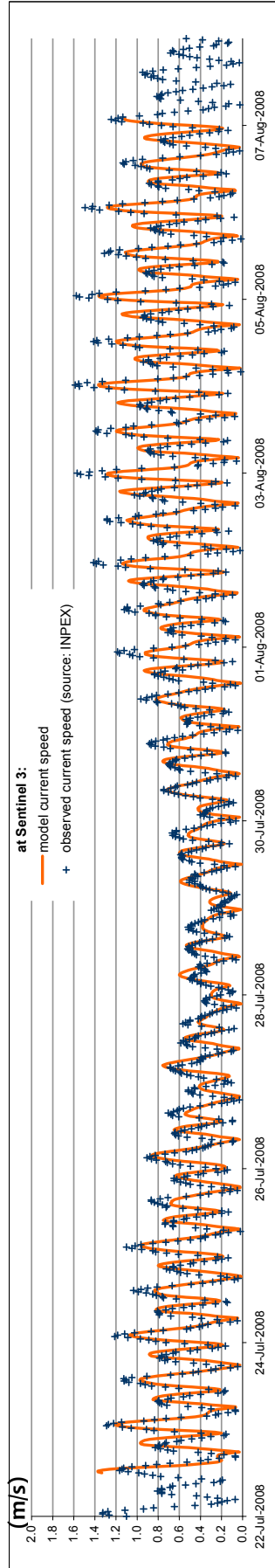


Figure 29 Current speed at Sentinel 3, Model comparison against observed data

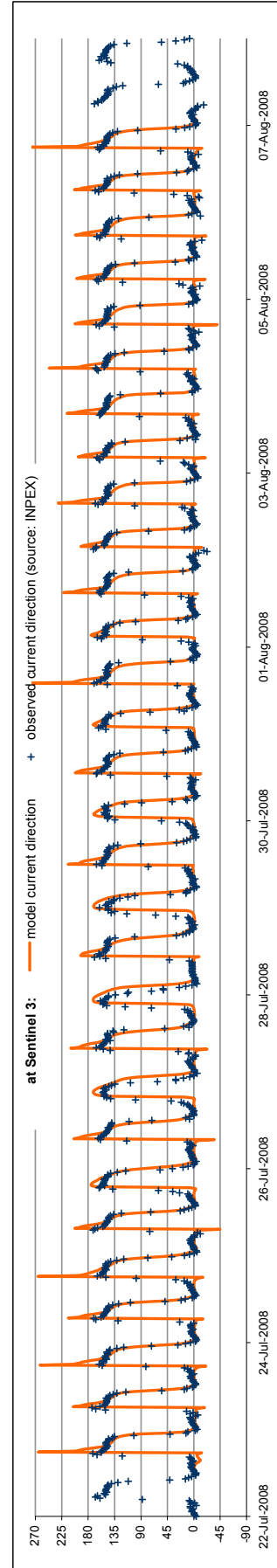


Figure 30 Current direction at Sentinel 3, Model comparison against observed data

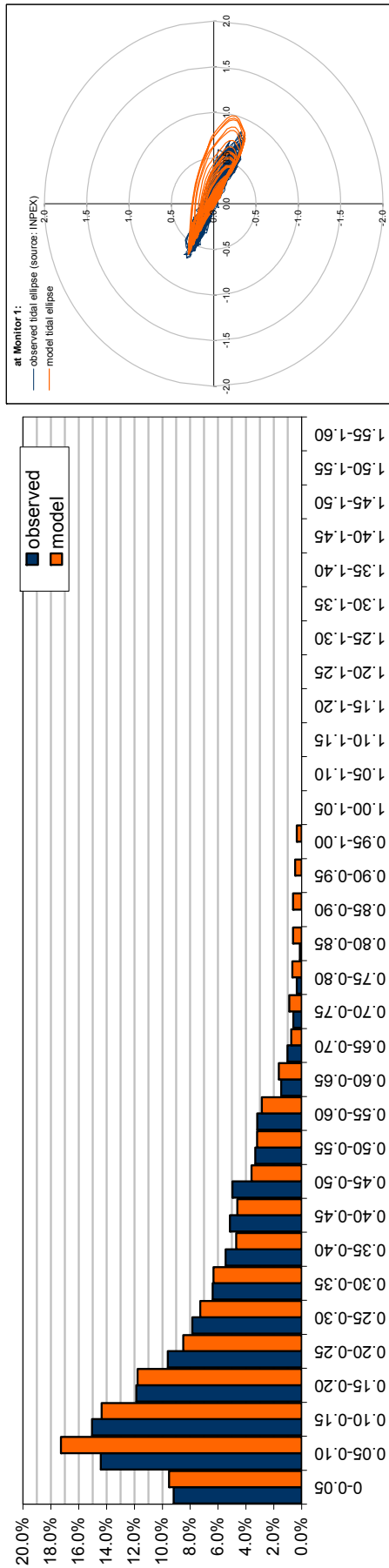


Figure 31 Current speed distribution and tidal ellipse at Monitor 1, Model comparison against observed data

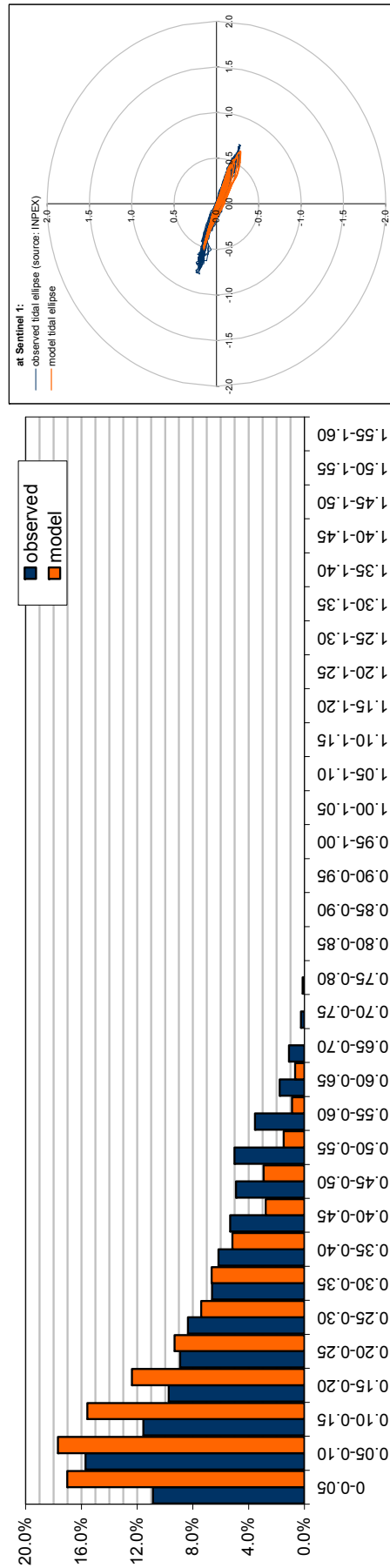


Figure 32 Current speed distribution and tidal ellipse at Sentinel 1, Model comparison against observed data

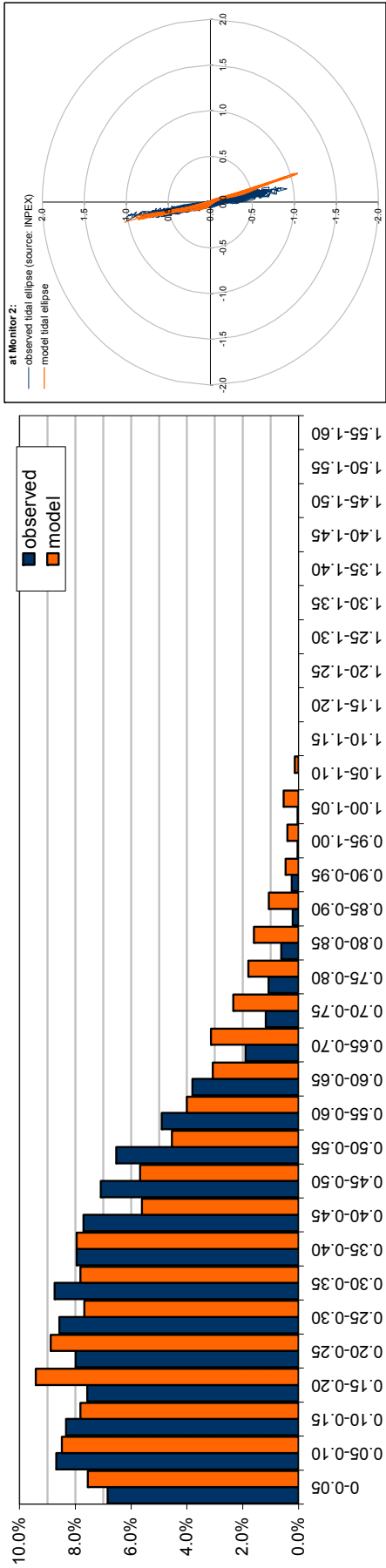


Figure 33 Current speed distribution and tidal ellipse at Monitor 2, Model comparison against observed data

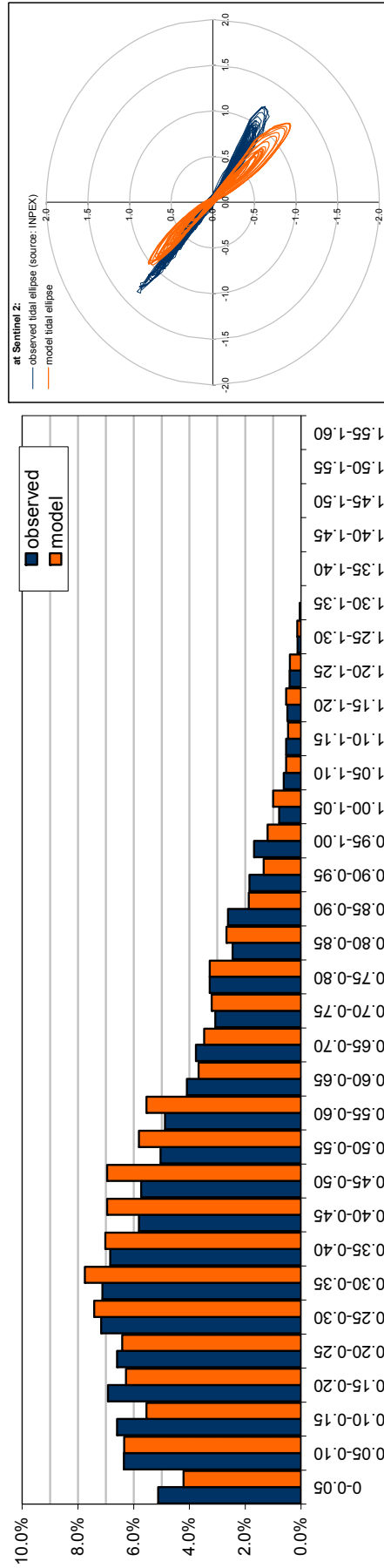


Figure 34 Current speed distribution and tidal ellipse at Sentinel 2, Model comparison against observed data

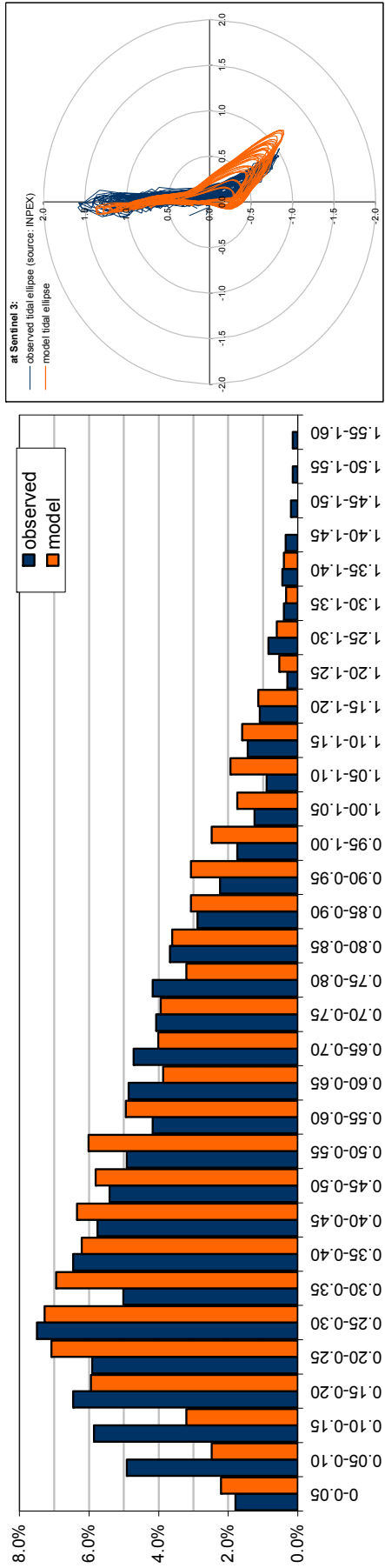


Figure 35 Current speed distribution and tidal ellipse at Sentinel 3, Model comparison against observed data

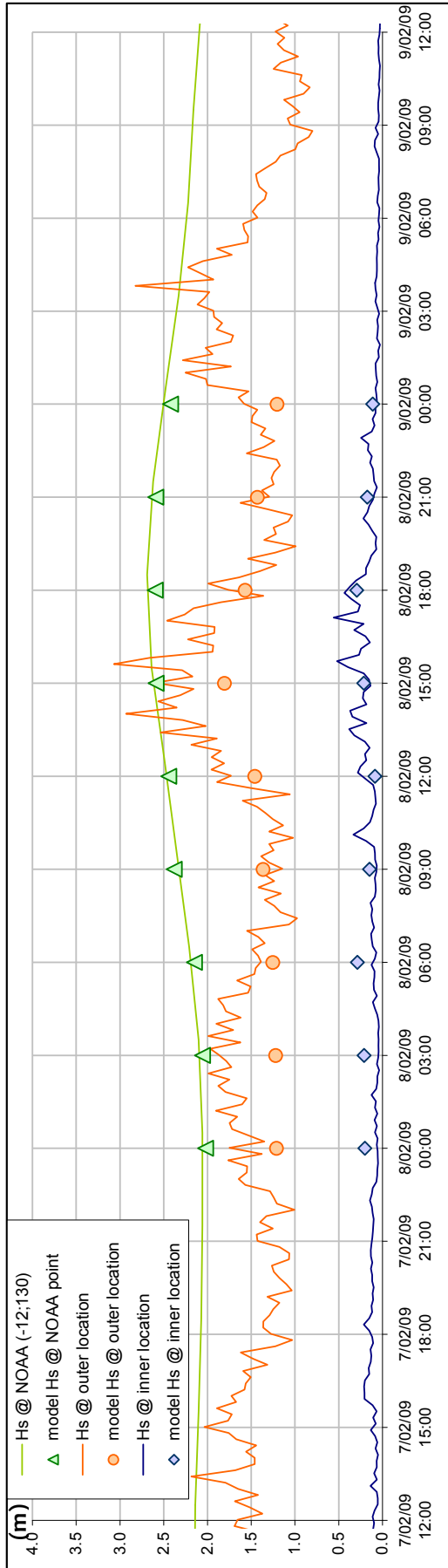


Figure 36 Significant wave height, Model comparison against observed data

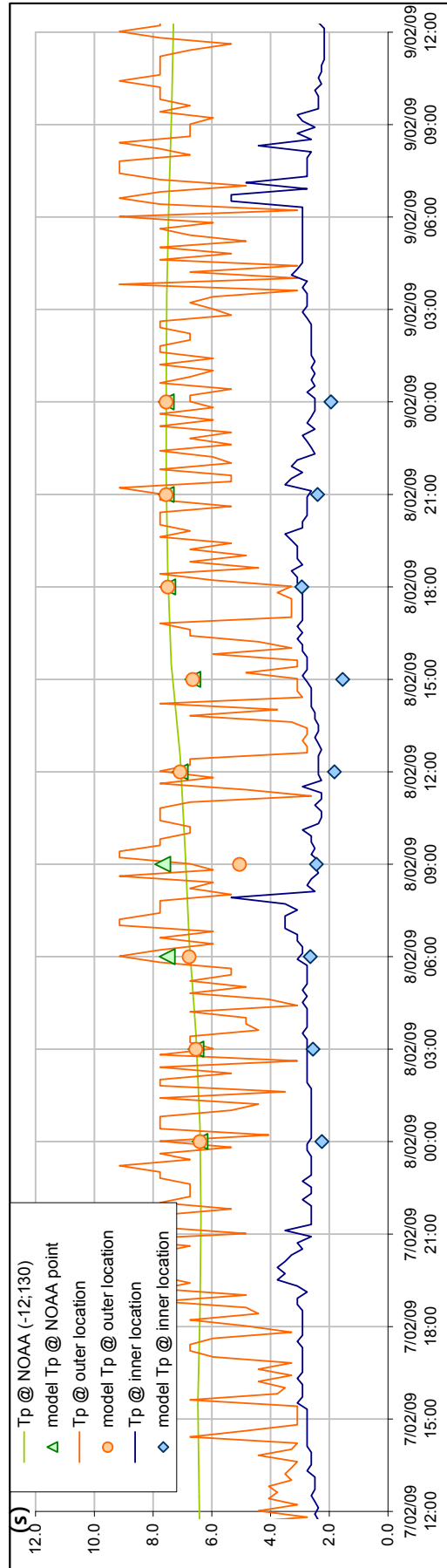


Figure 37 Absolute peak period, Model comparison against observed data

Appendices

Appendix 1 Numerical wave and flow solvers

TELEMAC is a state-of-the-art free surface flow suite of solvers developed by a kernel of European organisations including the Laboratoire National d'Hydraulique et Environnement of Electricité de France, the Federal Waterways Engineering and Research Institute of Germany and HR Wallingford in the UK. It is currently being used by more than 200 organisations worldwide.

The caption opposite shows the cover of the latest book (dated April 2007) published on this solver. This reference includes in particular a full description of the latest theoretical and numerical developments (reference below).

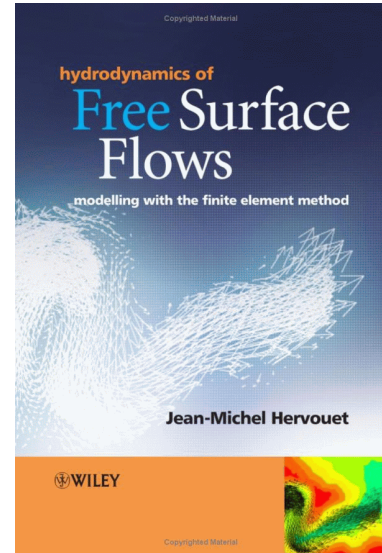
HR Wallingford has gained access to the entire source code for the last 15 years and counts experts in the use of the solver, offering applied research and specialist consultancy services in civil engineering and environmental hydraulics to clients worldwide.

TELEMAC two-dimensional module, TELEMAC-2D, solves the 2D depth-integrated shallow water equations and is used to model various hydraulic phenomena such as tidal flows in estuaries, coastal flows, storm surges, floods in rivers including turbulence structures resulting from flow obstructions and transcritical flows, dam break simulations, cooling water dispersion and infill of navigation channels. The three-dimensional module, TELEMAC-3D, solves the 3D Navier-Stokes equations either under hydrostatic or non-hydrostatic assumptions and is used to model hydraulic phenomena such as density currents, reservoir and estuary stratification and salt intrusion, lock exchanges and detailed assessment of tidal energy resources.

The TELEMAC system as a whole has been developed under a quality assurance system including the application of a standard set of validation tests.

Contrary to solvers used by other consultants, TELEMAC was designed from the outset, 20 years ago, to use the mathematically more advanced finite element techniques so that very flexible unstructured triangular meshes can be used. This is superior to using an orthogonal and/or curvilinear mesh as the engineer gains more control over mesh refinement particularly in cases of detached coastlines and manmade structures. In addition, currents that are tangential to solid or coastal boundary conditions (slip or nonslip conditions) are correct by design. The structure of the TELEMAC-3D mesh consists of prisms. The horizontal space is discretized using a triangular finite element mesh. The vertical space is discretized in a number of curved surfaces, referred to as “planes”, with sigma coordinates. The horizontal mesh is reproduced along the vertical following these planes to form the prisms.

The model can be run either in a Cartesian coordinate system when modelling small regions, part of rivers, estuaries and seas, with the possibility to apply a local Coriolis parameter, or on a spherical mesh for larger regions in which case the Coriolis parameter is computed from the latitude on the mesh. The effect of a wind blowing on the water surface and causing a set-up or wind induced current and the effect of an atmospheric pressure variation causing an inverted barometer effect can be included in the model. The bed friction can be specified with a Chezy, Strickler/Manning or linear coefficient, or a Nikuradse roughness length. It is possible to



define a spatially varying friction coefficient over the model area. Viscosity can be imposed as a given eddy viscosity value or a k-epsilon model can be used if needed.

TELEMAC-3D is driven by currents and/or water levels supplied at the open boundaries, and calculates water level at each node of the mesh, and the three components of velocity at each node and layer.

More detailed information about the solver can be found in the following references:

- Jean-Michel Hervouet, “Hydrodynamics of Free Surface Flows: Modelling with the Finite Element Method”, Wiley Blackwell, April 2007, 360p, ISBN-13: 978-0470035580.
- EDF-LNHE, “TELEMAC Modelling System, 2D Hydrodynamics, TELEMAC-2D Validation Document”, July 2000

Appendix 2 Characterisation of the Darwin Harbour mangrove

1. Introduction

The mangroves were included in this study's numerical models based on geo-referenced contour data supplied to HR Wallingford by INPEX, which accurately delineate vegetation units within Darwin Harbour mangrove (Ref. 1), and based on a description of the plants in the mangrove by the Department of Infrastructure, Planning and Environment (Ref. 6). A literature review was performed in this study (references in Section 4 of this Appendix) to determine how best to represent the effect of the vegetation on the flows as the tide rises and reaches the mangrove.

2. Darwin Harbour mangrove

MANGROVE PLANTS

Many plant growth forms are associated with mangrove ecosystems including vines, grasses, shrubs, chenopods, sedges, forbs, palms, ferns and parasitic plants. Nine tree species are deemed representative of the mangrove communities present in the Top End of the Northern Territory (Ref. 6). These species vary considerably in their appearance, adaptations to the coastal habitats and position in relation to the coast. They are:

Rhizophora stylosa (Stilt rooted mangrove)

- Tree between 5 and 12 m high
- Intertwined, arching roots that originate from the base and lower branches
- Found towards the seaward edge of mangrove communities



Bruguiera exaristata
(Orange mangrove)

- Spreading tree, between 3 and 10m high
- Buttressed trunks surrounded by many knee like pneumatophores
- Generally found in the landward zone of mangrove communities.



Ceriops tagal
(Yellow mangrove)

- Small trees or shrubs, between 2 and 6m high
- Base often buttressed
- Cannot tolerate high levels of inundation, therefore mainly found on the landward fringe of mangrove communities and in salt pan areas.



Sonneratia alba
(Mangrove apple)

- Spreading tree between 4 and 5 m high (can reach 8m)
- Large, cone shaped pneumatophores
- Can be found in the seaward zone.



Aegialitis annulata
(*Club mangrove*)

- Small shrub, generally does not exceed 1.5m but can reach 3m in height
- Thick trunk at the base that quickly narrows
- Found in a variety of habitats, including rocky beach environments in the seaward zone.



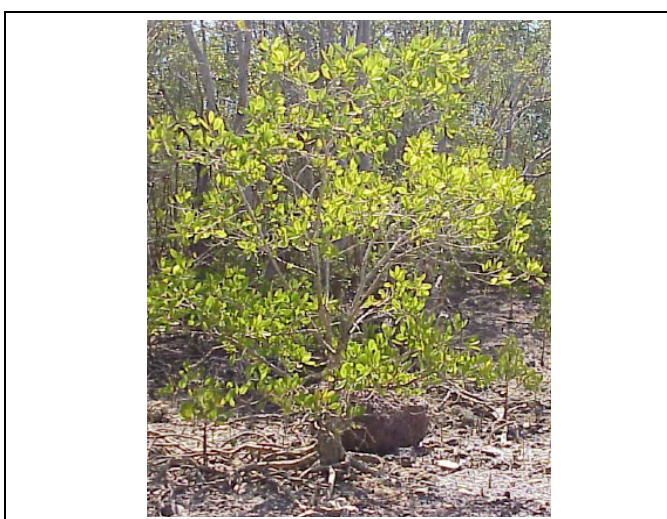
Avicennia marina
(*White or grey mangrove*)

- Most widespread mangrove in Australia
- Multi-stemmed tree between 4 and 10m high (can reach 25m)
- Found in varied environments including the upper tidal limit of estuaries, salt flats and along the seaward margin
- Pencil like pneumatophores.



Excoecaria ovalis
(*Blind your eye*)

- Small tree or shrub up to 4m high
- Roots occasionally knot above the soil surface
- Can be found in and around mudflats and in coastal mangrove communities.



Hibiscus tiliaceus
(*Beach hibiscus*)

- Small spreading tree which can reach 8m in height
- Frequently found in sandy beach areas but can also be found below the high tide mark.



Lumnitzera racemosa
(*Black mangrove*)

- Shrub or tree up to 5m high
- Generally found towards the landward edge of mangrove areas
- If found in salt pans, may remain below 1m high..



These nine species were considered for the purpose of this analysis. Additional details about these species are available from the report by the Department of Infrastructure, Planning and Environment (Ref. 6).

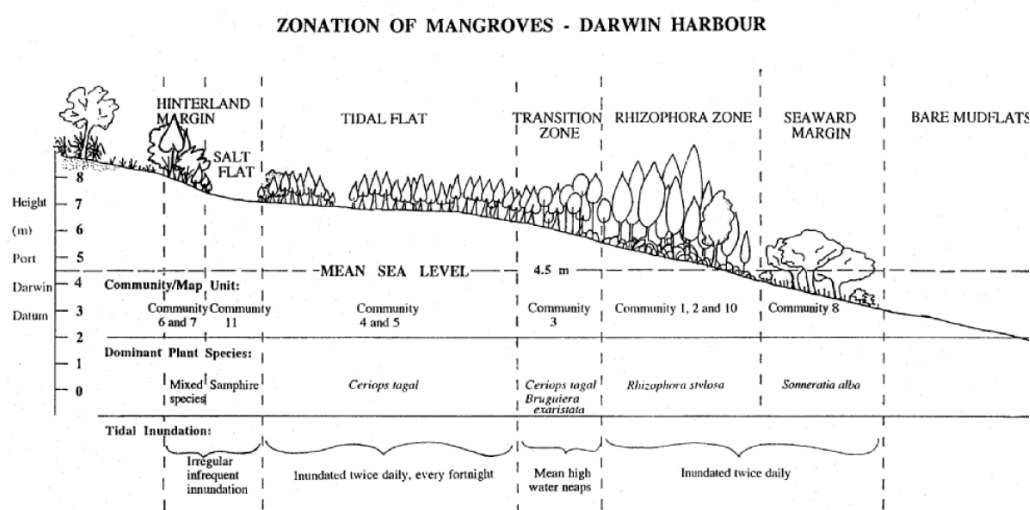
The table below presents their characteristics in terms of drag coefficient (C_d), diameter (m_t m) and density (D_t m⁻²) (see Section 3 of this Appendix). These characteristics were estimated in this study based on pictures (to help determine a representative diameter for each species) and aerial photographs (to help determine a representative density for each species).

	<i>Tree trunk</i>			<i>Root / Pneumatophores</i>		
	C_d ($$)	m_t (m)	D_t (m ²)	C_d ($$)	m_t (m)	D_t (m ²)
<i>Rhizophora stylosa</i>	1.2	0.1	0.5	1.2	0.02	10
<i>Bruguiera exaristata</i>	1.4	0.3	0.5	1.5	0.04	10
<i>Ceriops tagal</i>	1.4	0.3	0.5	-	-	-
<i>Sonneratia alba</i>	1.2	0.3	0.1	1.2	0.04	10
<i>Aegialitis annulata</i>	1.3	0.2	0.1	1.2	0.01	5
<i>Avitennia marina</i>	1.2	0.3	0.1	1.2	0.01	5
<i>Exoecaria ovalis</i>	1.4	0.1	0.1	-	-	-
<i>Hibiscus tiliaceus</i>	1.2	0.3	0.1	-	-	-
<i>Lumnitzera racemosa</i>	1.2	0.1	0.1	-	-	-

MANGROVE ZONATION

Mangrove communities are often made up of obvious zones which run parallel to the shore. Each zone is likely to be dominated by one particular tree species which has adapted to specific environmental characteristics. Generally a minimum of three zones are recognised,

these being the landward zone, the seaward zone and an intertidal zone (Ref. 3). The figure below shows a more complicated zonation pattern which has been mapped in Darwin Harbour (Ref. 7).



Schematic profile of mangrove zonation in Darwin Harbour (Ref. 7)

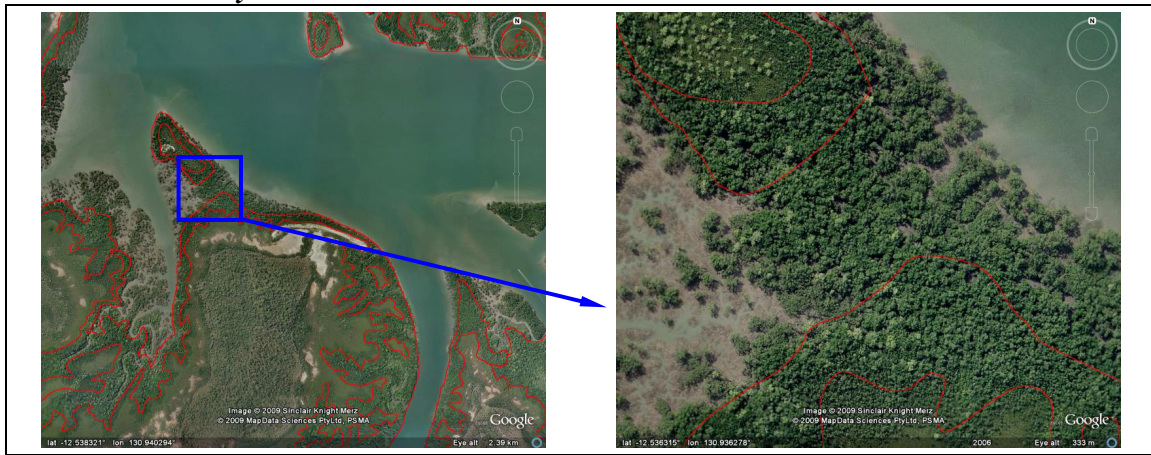
The geo-referenced contour data provided by INPEX included a total of twelve communities, where one or more tree species are present. These are:

Community	Description	Total area (m²)
1	<i>Mangrove Closed Forest</i> Rhizophora stylosa closed-forest/low closed forest (Shoreline forest)	7,078,560
2	Rhizophora stylosa/Campostemon schultzei closed-forest (tidal creek)	157,370,370
3	Rhizophora/Bruguiera/Ceriops closed-forests/open-forest (transition)	8,978,755
4	Ceriops tagal low closed-forest (mid tidal flat)	3,225,803,410
5	Ceriops tagal/Avicennia marina low closed forest (high tidal flat)	25,358,730
6	Mixed species low closed forest/open-forest (hinterland)	18,443,355
	<i>Mangrove Woodlands / Open Woodlands</i>	
7	Mixed species low woodland	4,955,700
8	Sonneratia alba woodland	11,481,285
9	Rhizophora stylosa low woodland (islands, rocky shores)	55,155
10	Low open-woodland (low tidal mudflat)	242,610
	<i>Salt flats</i>	
11	Samphire/Saltpan	18,286,895
	<i>Beach</i>	
12	Beach	281,965

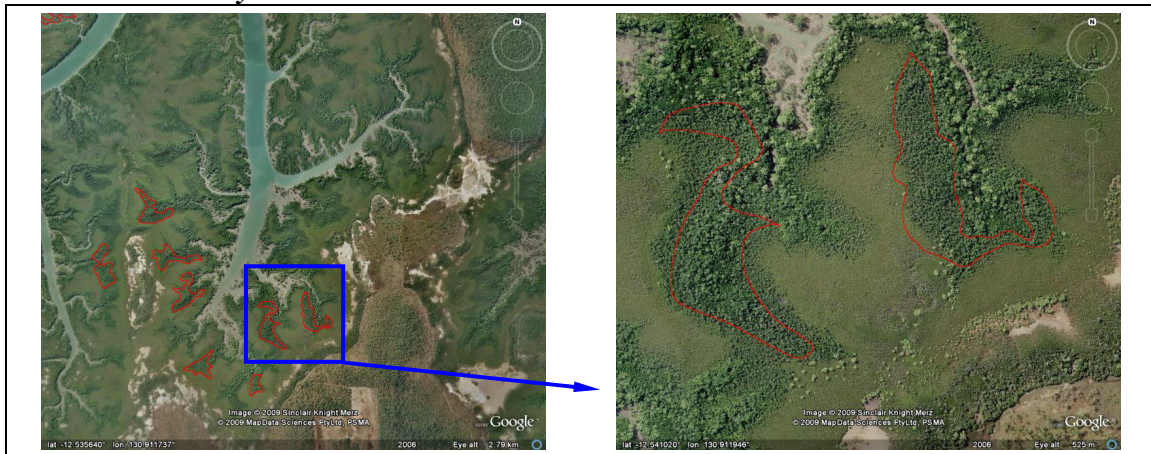
Community 1



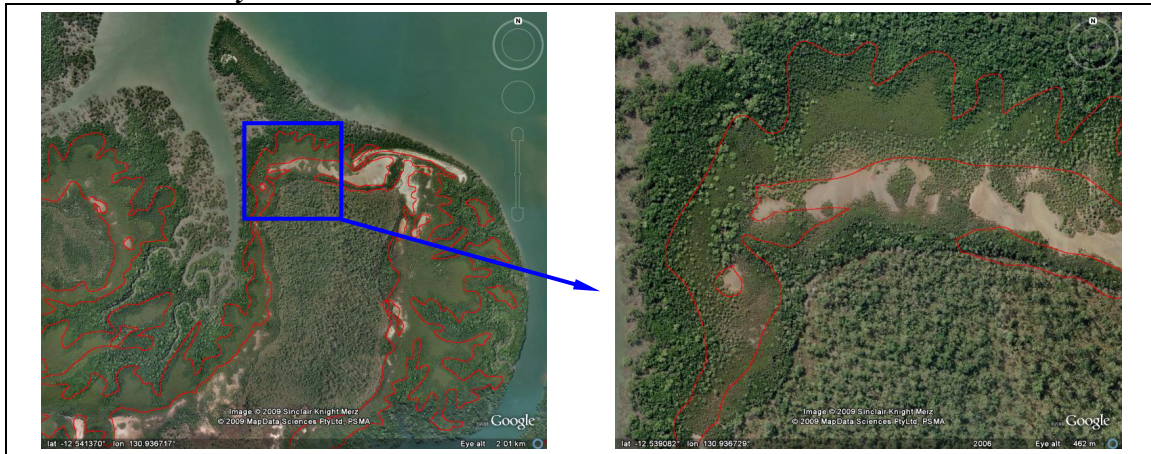
Community 2



Community 3



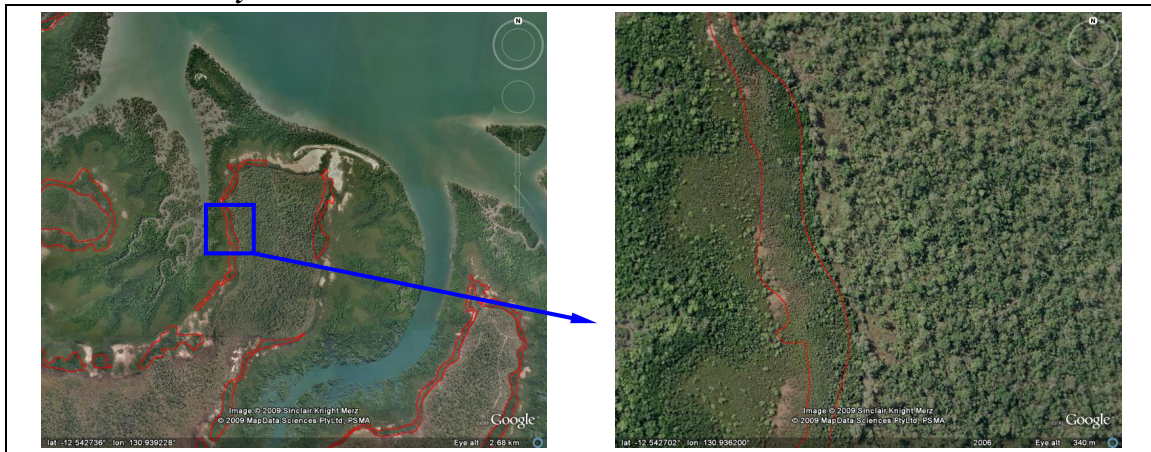
Community 4



Community 5



Community 6



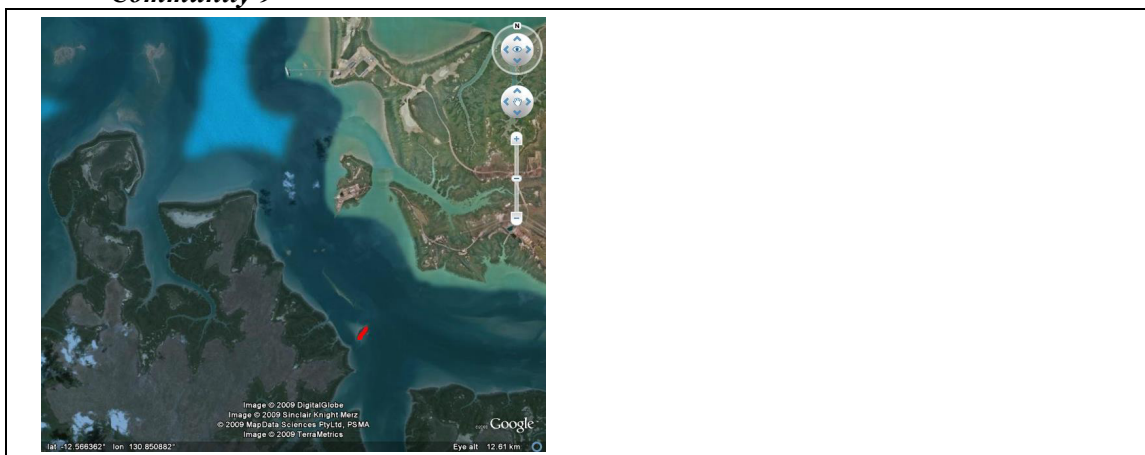
Community 7



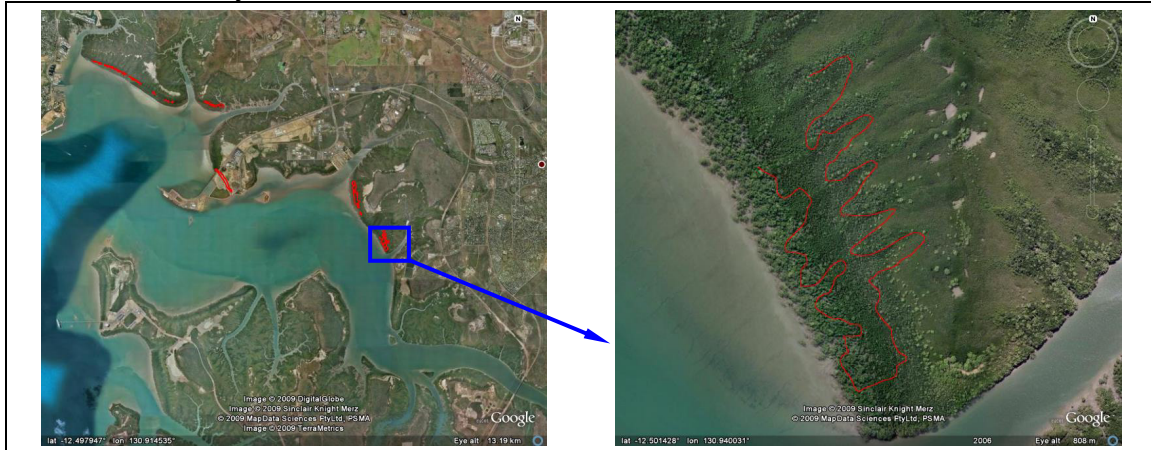
Community 8



Community 9



Community 10



Community 11



Community 12



3. Numerical representation of the mangrove

The drag coefficient (**D**) and the porosity (**P**) for each vegetation unit were estimated from the work conducted by Struve J. Falconer R. A., and Wu Y (Ref. 13, figure opposite).

It was initially envisaged to use a porosity factor as well as a friction factor in the flow model to represent the mangrove areas. This analysis, however, indicated that the reduction in cross-sectional area (or blockage) due to the presence of the vegetation (tree trunks) was minimal (lower than 2%, see table below). No porosity was therefore specified in the final model simulations.

The friction factor (in the form of a Chézy coefficient) was, however, adjusted to account for the drag caused by the vegetation, i.e. it is dependent on the D factor computed by Struve J. Falconer R. A., and Wu Y (Ref. 13).

The drag forces due to vegetation in x- and y-directions are

$$F_x = C_d D_t m_t \frac{Q_x \sqrt{Q_x^2 + Q_y^2}}{H} \quad (4)$$

$$F_y = C_d D_t m_t \frac{Q_y \sqrt{Q_x^2 + Q_y^2}}{H} \quad (5)$$

D

where C_d is the drag coefficient, D_t the density of trees per unit area and m_t is the diameter of trees.

In addition to the drag forces, the model accounts for the reduction in cross-sectional flow area due to vegetation by using a porosity factor θ (Wu et al., 2001)

$$\theta = 1 - \pi \frac{D_t^2 m_t}{4} \quad (6)$$

P

$1 - \pi \frac{D_t m_t^2}{4}$

The table below gives revised values for each vegetation unit identified from the geo-referenced contour data supplied by INPEX (Ref. 1).

		<i>Communities</i>											
		1	2	3	4	5	6	7	8	9	10	11	12
<i>Species</i>	<i>Rhizophora stylosa</i>	1/3	1/3	1/5	-	-	-	-	-	1/3	-	-	-
	<i>Bruguiera exaristata</i>	-	-	1/5	-	-	-	-	-	-	-	-	-
	<i>Ceriops tagal</i>	-	-	1/5	1/3	1/4	-	-	-	-	-	-	-
	<i>Sonneratia alba</i>	-	-	-	-	-	-	-	1/4	-	-	-	-
	<i>Aegialitis annulata</i>	-	-	-	-	-	1/3	-	1/4	-	-	-	1/4
	<i>Avicennia marina</i>	-	-	-	-	1/4	-	1/4	-	-	-	-	1/4
	<i>Exoecaria ovalis</i>	1/3	1/3	1/5	1/3	1/4	1/3	1/4	1/4	1/3	1/2	1/2	1/4
	<i>Hibiscus tiliaceus</i>	1/3	1/3	1/5	1/3	1/4	1/3	1/4	1/4	1/3	1/2	1/2	1/4
	<i>Lumnitzera racemosa</i>	-	-	-	-	-	-	1/4	-	-	-	-	-
	D	0.12	0.12	0.27	0.09	0.09	0.05	0.04	0.16	0.12	0.03	0.03	0.06
P (%)	100	100	98	99	99	100	100	99	100	100	100	100	
Chézy	16	16	12	17	15	18	20	15	16	21	21	16	

Even though best judgement was applied in this analysis and the resulting friction coefficients are within appropriate physical ranges, there remains some degree of uncertainty. A sensitivity analysis to the value of the friction coefficient used for the mangrove in the numerical model was therefore conducted. Its conclusions are presented in Section 5.3 of the report.

4. References

- Ref. 1. Geo-referenced contour data of the mangrove, INPEX
inpex_gis_GISADMIN_ENVR_NTY_NtGovtData_NRT_20080221_M52_Mangrove
sDarwinHarbour25k.shp
August 2009.
- Ref. 2. Brocklehurst P. S., Edmeades B. “Regionalisation of mangrove communities along the Northern Territory Coast” Technical Memorandum No. 96/17
Department of Lands, Planning and Environment, Darwin. 1996.
- Ref. 3. Claridge D., Burnett J. “Mangroves in focus” Wet Paper Marine Education, Ashmore. 1993.
- Ref. 4. Copeland R. R. “Determination of flow resistance coefficients due to shrubs and woody vegetation”. US Army Corps of Engineers
Technical Note ERDC/CHL CHETN-VIII-3. 2000.
- Ref. 5. Fathi-Maghadam M., Kouwen N. “Non rigid, non submerged, vegetative roughness on floodplains” Journal of hydraulic engineering,
Vol. 123, No. 1, pp 51-57. 1997.
- Ref. 6. Lee, G. P. “Mangroves in the Northern Territory” Department of Infrastructure, Planning and Environment, Darwin. Report Number 25/2003D. 2003.
- Ref. 7. Liu W.-C., Hsu M.-H., Wang C.-F. “Modeling of flow resistance in mangrove swamp at mouth of tidal Keelung River, Taiwan” Journal of Waterways,
Port, Coastal and Ocean Engineering, Vol. 129, No. 2. 2003.
- Ref. 8. Metcalfe K. “Mangrove litter production, Darwin Harbour NT - A study of litter fall as a measure of primary production in the mangrove communities of Darwin Harbour” Masters thesis, Northern Territory University, Darwin. 1999.
- Ref. 9. Naot D., Nezu I., Nakagawa H. “Hydrodynamic behaviour of partly vegetated open channels” Journal of hydraulic engineering,
Vol. 122, No. 11, pp 625-633. 1996.
- Ref. 10. Nepf H. M. “Drag, turbulence and diffusion in flow through emergent vegetation” Water Resources Research, Vol. 35, No. 2, pp 479-489. 1999.
- Ref. 11. Nepf H. M., Vivoni E. R. “Flow structure in depth-limited, vegetated flow” Journal of geophysical Research, Vol. 105, No. C12, pp 28547-28557. 2000.
- Ref. 12. Rigo D., Chacaltana J. T. A. “Computational modelling of mangrove effects on the hydrodynamics of Vitoria Bay, Espirito Santo – Brazil”
Journal of Coastal Research, Special Issue 39, pp 1543-1545. 2006.
- Ref. 13. Struve J., Falconer R. A., Wu Y. “Influence of model mangrove trees on the hydrodynamics in a flume” Estuarine Coastal and Shelf Science,
Vol. 58, pp 163-171. 2003.

- Ref. 14. Water Monitoring Branch. “The health of the aquatic environment in the Darwin Harbour region.” Report 5/2005D.
Natural Resource Management Division. Department of Natural Resources, Environment and the Arts, Darwin. 2005.
(<http://www.nt.gov.au/nreta/water/aquatic/darwinharbour/>)
- Ref. 15. Wu F.-C., Shen H. W., Chou Y.-J. “Variation of roughness coefficients for unsubmerged and submerged vegetation” *Journal of Hydraulic Engineering*, Vol. 125, No. 9, pp 934-941. 1999.
- Ref. 16. Wu Y., Falconer R. A., Struve J. “Mathematical modelling of tidal currents in mangrove forests” *Environmental Modelling & Software*, 16, pp 19-29. 2001, Vol. 125, No. 9, pp 934-941. 1999.
- Ref. 17. “Fact Sheet, Mangrove Monitoring” Department of Natural Resources, Environment and the Arts, Darwin.
(http://www.nt.gov.au/nreta/natres/natveg/vegmapping/pdf/mangroves_darwin_harbour.pdf)
- Ref. 18. “Mangrove mapping of Darwin Harbour – Dataset summary” Department of Natural Resources, Environment and the Arts, Darwin.
(<http://www.nt.gov.au/nreta/natres/natveg/vegmapping/pdf/mangrovedarwin.pdf>)